ON GRASPING AND DYNAMIC COORDINATION OF MULTIFINGERED ROBOT HANDS

by

Zexiang Li, Ping Hsu, and Shankar Sastry

Memorandum No. UCB/ERL M87/63

15 September 1987

ON GRASPING AND DYNAMIC COORDINATION OF MULTIFINGERED ROBOT HANDS

by

Zexiang Li, Ping Hsu, and Shankar Sastry

Memorandum No. UCB/ERL M87/63

15 September 1987

ELECTRONICS RESEARCH LABORATORY

College of Engineering
University of California, Berkeley
94720

TITLE PAGE

ON GRASPING AND DYNAMIC COORDINATION OF MULTIFINGERED ROBOT HANDS

by

Zexiang Li, Ping Hsu, and Shankar Sastry

Memorandum No. UCB/ERL M87/63

15 September 1987

ELECTRONICS RESEARCH LABORATORY

College of Engineering
University of California, Berkeley
94720

On Grasping and Dynamic Coordination of Multifingered Robot Hands

Zexiang Li, Ping Hsu and Shankar Sastry

Electronics Research Laboratory
and Department of Electrical Engineering and Computer Sciences
University of California, Berkeley. Ca.94720

Abstract

This paper treats two fundamental problems in the kinematics and the control of multifingered robot hands: grasp planning and the determination of coordinated control laws. We develop dual notions of grasp stability and manipulability and use these notions to formulate grasp quality measures. We give a control law for the coordinated control of a multifingered robot hand which takes into account both the dynamics of the object and the fingers and assumes a point contact model.

Table of Contents

1. Introduction:

A new avenue of progress in the area of robotics is the use of a multifingered robot hand for fine motion manipulation. The versatility of robot hands accrues from the fact that fine motion manipulation can be accomplished through relatively fast and small motions of the fingers and from the fact that they can be used on a wide variety of different objects (obviating the need for a large stockpile of custom end effectors). Several articulated hands such as the JPL/Stanford hand [10], the Utah/MIT hand [19] have recently been developed to explore problems relating to the grasping and manipulation of objects. It is of interest to note that the coordinated action of multiple robots in a single manufacturing cell may be treated in the same framework as a multifingered hand.

Grasping and manipulation of objects by a multifingered robot hand is more complicated than the manipulation of an object rigidly attached to the end of a six-axis robotic arm for two reasons: the kinematic relations between the finger joint motion and the object motion are complicated, and the hand has to firmly grasp the object during its motion.

The majority of the literature in multifingered hands has dealt with kinematic design of hands and the automatic generation of stable grasping configurations as also with the use of task requirement as a criterion for choosing grasps (see for example the references [1 ~ 4], [6 ~ 8], [10], [13 ~ 18]). Some of these references ([2,3,6,12,14,16]) have suggested the use of a task specification as a criterion for choosing a grasp, albeit in a some what preliminary form. A few control schemes for the coordination of a multifingered robot hand or a multiple robot system have been proposed in ([8, 23 ~ 26]). The most developed scheme is the master-slave methodology ([23,24]) for a two-manipulator system. The schemes developed so far all suffer from the drawback that they either assume rigid attachment of the fingertips to the object or are open loop. The schemes do not account for an appropriate contact model between the fingertips and the object.

This paper treats two fundamental problems in the kinematics and control of multifingered hands: *grasp planning and the determination of coordinated control laws.* We develop dual notions of grasp stability and manipulability and use these notions to formulate grasp quality measures (this constitutes an extension of our earlier work in [2]). We give a control law for the coordinated control of a multifingered robot hand which takes into account both the dynamics of the object and the fingers and assumes a point contact model.

A brief outline of the paper is as follows:

In section 2, we define the grasp map and its associated effective force domain, and the hand Jacobian. We develop dual generalized force and velocity transformation formulae relating the finger joint

torques and velocities to the generalized force on and generalized velocity of the body being manipulated. Using these relations we define stability and manipulability of a grasp. In section 3, we extend our previous work in [2] to define task oriented measures for grasp stability and manipulability. In section 4, we use the machinery in sections 2 and 3 to develop a new "computed torque-like" control scheme for the dynamic coordination of the multifingered robot hand, along with a proof of its convergence.

2. Mathematical Background

2.1. Transformation Relations for Rigid Body Motions in R^3

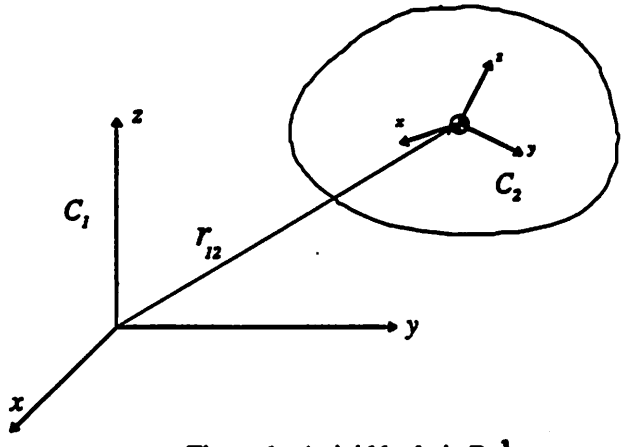

Figure 1. A rigid body in R^3.

Let C_1, C_2 be the two coordinate frames in R^3 as shown in Figure 1. Let r_{12} be the vector representing the origin of C_2 in the C_1 frame and $A_{12} \in R^{3\times3}$ be the unit x, y, z vectors of the C_2 coordinate frame in the C_1 frame. It follows that A_{12} is an unitary matrix with determinant +1, i.e., $A_{12} \in SO(3)$, and that if a point p has coordinates p_2 in the C_2 frame, its coordinates are $A_{12}p_2 + r_{12}$ in the C_1 frame, and conversely that coordinates p_1 in the C_1 frame transform to $A_{12}^t p_1 - A_{12}^t r_{12}$ in the C_2 frame. These facts are conveniently expressed by means of homogeneous coordinates [20] by appending the scalar 1 to the coordinates of p_1 and noticing that

$$\begin{bmatrix} p_1 \\ 1 \end{bmatrix} = \begin{bmatrix} A_{12} & r_{12} \\ 0 & 1 \end{bmatrix} \begin{bmatrix} p_2 \\ 1 \end{bmatrix}. \tag{2.1-1}$$

Transformation matrices of the form

$$g_{12} = \begin{bmatrix} A_{12} & r_{12} \\ 0 & 1 \end{bmatrix} \tag{2.1-2}$$

with $A_{12} \in SO(3)$, $r_{12} \in R^3$ constitute the Euclidean group $SE(3)$ or the group of rigid body motions in R^3, isomorphic to the group $R^3 \times SO(3)$. The group operation in $SE(3)$ is the usual matrix multiplication. Thus, if C_3 were the third coordinate frame with g_{23} representing the transformation from C_3 coordinates to C_2 coordinates, then,

$$g_{13} = g_{12} g_{23} \tag{2.1-3}$$

with g_{13} being the transformation relating C_3 coordinates to C_1 coordinates. Also

$$g_{21} = g_{12}^{-1} \tag{2.1-4}$$

The added payoff of the so-called homogeneous coordinates of (2.1-2) for the Euclidean group is that they can be used to represent rigid body motions in R^3. Thus, if in Figure 1 the coordinate frame C_2 is attached to the rigid body, then the configuration of the rigid body may be described by the matrix g_{12} of (2.1-2), with A_{12} representing the orientation of the body and r_{12} representing the position of the origin of the body coordinate frame C_2. To describe the differential motion of the body, consider a trajectory of the body, parametrized by a C^1-curve g_{12}: $[0, t_0) \to SE(3)$, where $[0, t_0)$ is the time interval. Differentiating it we obtain

$$\dot{g}_{12}(t) = \begin{bmatrix} \dot{A}_{12}(t) & \dot{r}_{12}(t) \\ 0 & 0 \end{bmatrix} \in T_{g_{12}} SE(3) \tag{2.1-5}$$

where $T_{g_{12}} SE(3)$ denotes the tangent space to $SE(3)$ at g_{12}, and $\dot{A}_{12}$ satisfies

$$\dot{A}_{12}^t A_{12} + A_{12}^t \dot{A}_{12} = 0 \tag{2.1-6}$$

((2.1-6) is obtained by differentiating $A_{12}^t A_{12} = I$). Thus, $A_{12}^t \dot{A}_{12}$ is a skew-symmetric matrix of the form

$$A_{12}^t \dot{A}_{12} = \begin{bmatrix} 0 & -\omega_3 & \omega_2 \\ \omega_3 & 0 & -\omega_1 \\ -\omega_2 & \omega_1 & 0 \end{bmatrix} \triangleq S(\omega_{12}) \tag{2.1-7}$$

with $\omega_{12} = (\omega_1, \omega_2, \omega_3)^t$. It is easy to verify that the operator S which takes a vector in R^3 to the skew-symmetric matrix satisfies

$$S(\omega) \cdot f = \omega \times f \qquad \text{for all } \omega, f \in R^3 \tag{2.1-8}$$

and

$$AS(\omega)A^t = S(A\omega) \qquad \text{for all } A \in SO(3). \tag{2.1-9}$$

We define $\omega_{12} = S^{-1}(A_{12}^t \dot{A}_{12})$ to be the *rotational velocity* and $v_{12} = A_{12}^t \dot{r}_{12}$ the *translational velocity* of the moving rigid body. Thus, a generalized velocity of the body is of the form $(v_{12}^t, \omega_{12}^t)^t$ and it follows that

$$\begin{bmatrix} S(\omega_{12}) & v_{12} \\ 0 & 0 \end{bmatrix} = g_{12}^{-1} \cdot \dot{g}_{12}. \tag{2.1-10}$$

It is obtained by left multiplying (2.1-5) by g_{12}^{-1}.

Remark: The generalized velocity defined in (2.1-10) is the instantaneous velocity of the body frame C_2 expressed in the *body coordinates*. The reader should compare this definition with the convention of representing the body velocity in the *inertial coordinates*, which is given by right multiplying (2.1-5) by g_{12}^{-1}.

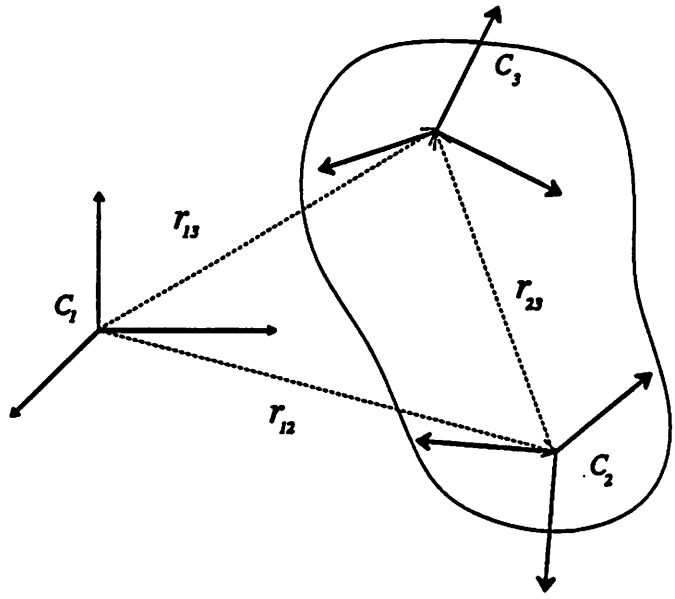

Figure 2

Consider now that a second coordinate frame C_3 fixed to the body which is also used to describe the motion of the rigid body (see Figure 2). Let the trajectory of C_3 be

$$g_{13} = \begin{bmatrix} A_{13} & r_{13} \\ 0 & 1 \end{bmatrix} \tag{2.1-11}$$

and its generalized velocity be $(v_{13}^t, \omega_{13}^t)^t$. If the relative displacement of C_3 from C_2 is given by the *constant* transformation

$$g_{23} = \begin{bmatrix} A_{23} & r_{23} \\ 0 & 1 \end{bmatrix}, \qquad \dot{g}_{23} = 0 \tag{2.1-12}$$

the generalized velocities $(v_{13}^t, \omega_{13}^t)^t$ and $(v_{12}^t, \omega_{12}^t)^t$ are related by the following transformation

$$\begin{bmatrix} v_{13} \\ \omega_{13} \end{bmatrix} = \begin{bmatrix} A_{23}^t & -A_{23}^t S(r_{23}) \\ 0 & A_{23}^t \end{bmatrix} \begin{bmatrix} v_{12} \\ \omega_{12} \end{bmatrix} \tag{2.1-13}$$

To see this, we observe that

$$g_{13} = g_{12} g_{23} = \begin{bmatrix} A_{12}A_{23} & A_{12}r_{23} + r_{12} \\ 0 & 1 \end{bmatrix} \tag{2.1-14}$$

from which we obtain that

$$S(\omega_{13}) = (A_{12}A_{23})^t (\dot{A}_{12}A_{23}) = S(A_{23}^t \omega_{12}) \tag{2.1-15a}$$

and

$$v_{13} = (A_{12}A_{23})^t(\dot{A}_{12}r_{23} + \dot{r}_{12}) = -A_{23}^t\, S(r_{23})\omega_{12} + A_{23}^t v_{12}. \tag{2.1-15b}$$

Combining (2.1-15a) and (2.1-15b) gives (2.1-13). Hence, the generalized velocities of a rigid body described using different coordinate frames are related by the constant linear transformations (2.1-13).

We denote the space of generalized velocity of the rigid body at the identity configuration by $T_eSE(3)$, and notice that an element $\dot{g} \in T_gSE(3)$ is pulled back to an element of $T_eSE(3)$ by left multiplying (2.1-5) by g^{-1} (2.1-10). Dual to $T_eSE(3)$ is the space of generalized forces (or wrenches) that can be exerted on the rigid body, and we denote it by $T_e^*SE(3)$. In the body coordinate frame, we can write a generalized force (or a wrench) $\eta \in T_e^*SE(3)$ as

$$\eta = \begin{bmatrix} f_b \\ m_b \end{bmatrix} \tag{2.1-16}$$

where $f_b, m_b \in R^3$ are respectively the force and the moment exerted on the body. The work done per unit time of η on a generalized velocity $(v^t, \omega^t)^t$ is given by

$$[f_b^t, m_b^t]\cdot\begin{bmatrix} v \\ \omega \end{bmatrix} = f_b^t v + m_b^t \omega \tag{2.1-17}$$

Similarly, when a second body coordinate frame C_3 is used to described the motion of the rigid body, we denote the set of generalized forces expressed in the C_3 frame by $\eta_{13} = (f_{b,13}^t, m_{b,13}^t)^t$. The wrench transformation between $\eta_{12} = (f_{b,12}^t, m_{b,12}^t)^t$ and η_{13} are given by the dual relation of (2.1-13), using the principle of virtual work (2.1-17), as

$$\begin{bmatrix} f_{b,12} \\ m_{b,12} \end{bmatrix} = \begin{bmatrix} A_{23} & 0 \\ S(r_{23})A_{23} & A_{23} \end{bmatrix}\begin{bmatrix} f_{b,13} \\ m_{b,13} \end{bmatrix} \tag{2.1-18}$$

(2.1-13) and its dual (2.1-18) are the basic transformation relations to be used in this paper.

When we study grasping and manipulation by a multifingered robot hand, C_2 will be used to denote the body frame fixed to the center of mass, and C_3 the contact frame fixed to the contact point between the fingertip and the object.

2.2 The Grasp Map G and the Hand Jacobian J_h

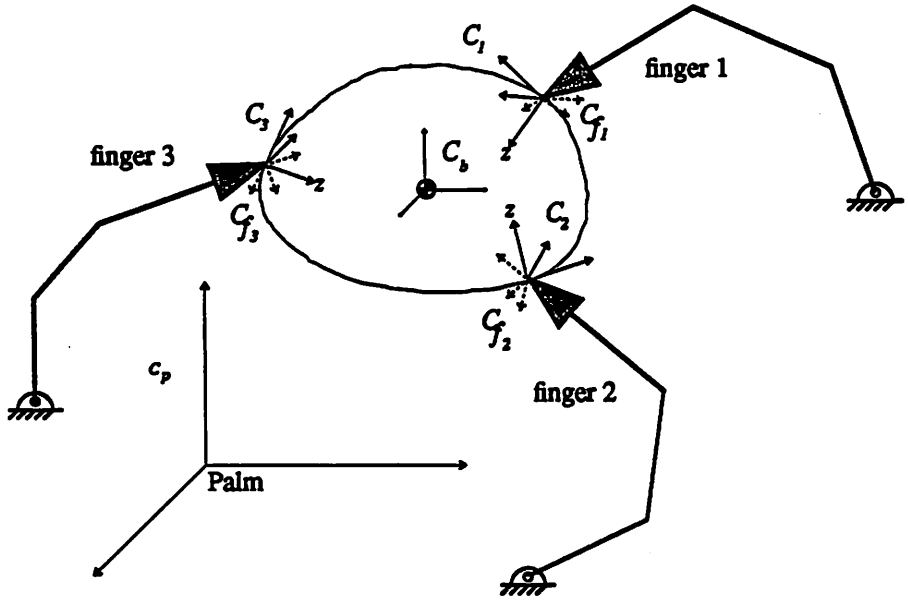

Figure 3. A three-fingered hand grasping an object.

Figure 3 shows a three fingered hand grasping an object. There are four sets of coordinate frames associated with the hand: a palm frame C_p, fingertip frames C_{f1}, C_{f2}, C_{f3}, associated with each of the fingertips, contact frames C_1, C_2, C_3 associated with each contact point on the object, and a body coordinate frame C_b fixed to the mass center of the object and oriented so that the moment of inertia matrix of the object is diagonal. The coordinate frame C_i, i=1,2,3 are chosen so that the z-axis coincides with the inward pointing normal to the body at the point of contact. In the following, the relative motion of a frame C_b with respect to a frame C_a will be denoted by

$$g_{ab} = \begin{bmatrix} A_{ab} & r_{ab} \\ 0 & 1 \end{bmatrix}, \quad A_{ab} \in SO(3),\ r_{ab} \in \mathrm{R}^3 \tag{2.2-1}$$

For example,

$$g_{pf_i} = \begin{bmatrix} A_{pf_i} & r_{pf_i} \\ 0 & 1 \end{bmatrix}$$

represents the relative motion of the i th fingertip frame with respect to the palm frame. Similarly, we denote by $(v_{ab}^t, \omega_{ab}^t)^t$ the generalized velocity of frame C_b with respect to C_a.

In this paper, we use three commonly accepted contact models to model the contact between the fingertips and the object: (a) a point contact without friction, (b) a point contact with friction, and (c) a soft finger contact. It is well understood that the number of independent finger

wrenches that can be applied to the object through the contact is one for a point contact without friction (a force in the normal direction), three for a point contact with friction (a normal force and two frictional components in the tangential directions), and four for a soft finger contact (the three independent directions for a point contact with friction along with a torque in the normal direction).

Let n_i be the number of independent contact wrenches that can be applied to the body through the ith contact and $T_e^*SE(3)$ the wrench space of the object. Consider the following definition.

Definition 2.1 (contact): *A contact on a rigid body is a map* $\psi_i : \mathrm{R}^{n_i} \to T_e^*SE(3)$ *given by*

$$\psi_i : \begin{bmatrix} x_{i1} \\ \cdot \\ \cdot \\ \cdot \\ x_{in_i} \end{bmatrix} \to \begin{bmatrix} A_{bi} & 0 \\ S(r_{bi})A_{bi} & A_{bi} \end{bmatrix} B_i \begin{bmatrix} x_{i1} \\ \cdot \\ \cdot \\ \cdot \\ x_{in_i} \end{bmatrix} = T_{fi} B_i \begin{bmatrix} x_{i1} \\ \cdot \\ \cdot \\ \cdot \\ x_{in_i} \end{bmatrix} \tag{2.2-2}$$

Here T_{fi} is the transformation matrix specified in (2.1-18), and $B_i \in \mathrm{R}^{6 \times n_i}$ is the basis matrix which expresses the unit contact wrenches in the contact frame. For example, for a soft finger contact we have that

$$B_i = \begin{bmatrix} 0 & 0 & 1 & 0 \\ 0 & 1 & 0 & 0 \\ 1 & 0 & 0 & 0 \\ 0 & 0 & 0 & 0 \\ 0 & 0 & 0 & 0 \\ 0 & 0 & 0 & 1 \end{bmatrix} \tag{2.2-3}$$

Here the first column of B_i denotes the normal force applied to the object, the second and the third denote the frictional forces and the last column denotes the normal torque for the soft finger contact. Thus, $B_i x_i$ denotes the finger wrenches expressed in the contact frame.

When a multifingered hand consists of k fingers with each finger contacting the object at a point p_i with contact map $\psi_i : \mathrm{R}^{n_i} \to T_e^*SE(3)$ the grasp map for the hand is defined to be

Definition 2.2 (grasp map): *The grasp map for a k-fingered robot hand holding an object is a map* $G : \mathrm{R}^n \to T_e^*SE(3)$, $n = \sum_{i=1}^{k} n_i$ *given by*

$$G(x_{11},\cdots,x_{1n_1},\ x_{21},\cdots,x_{kn_k}) = \psi_1(x_1)+\cdots+\psi_k(x_k) \tag{2.2-4}$$

$$= \begin{bmatrix} T_{f1},\cdots,T_{fk} \end{bmatrix} \begin{bmatrix} B_1 & 0 & \ldots & 0 & 0 \\ 0 & B_2 & \ldots & . & . \\ . & 0 & \ldots & . & . \\ . & . & \ldots & 0 & . \\ . & . & \ldots & B_{k-1} & 0 \\ 0 & 0 & \ldots & 0 & B_k \end{bmatrix} \begin{bmatrix} x_1 \\ . \\ . \\ . \\ x_k \end{bmatrix} = T_f B x$$

Remarks: (1) The grasp map G transforms the applied finger wrenches expressed in the contact frames into the body wrenches in the body frame.

(2) Since a normal contact force can only be exerted unidirectionally and friction forces are finite in magnitude of size less than the normal force times the coefficient of friction, the domain of the grasp map needs to be restricted to a proper subset of R^n. For example, for a soft finger contact the effective force domain is

$$K_i = \{\ (x_{i1},\cdots x_{i4}) \in R^4,\ x_{i1} \geq 0, x_{i2}^2 + x_{i3}^2 \leq \mu_t^2 x_{i1}^2 \ \text{ and } \ |x_{i4}| \leq \mu_t\, x_{i1}\ \}$$

where μ_t, μ_t are the Coulomb, torsional friction coefficients respectively. The effective force domain for a point contact with and without friction are easily defined similarly and are convex cones in R^1 and R^3 respectively. The effective force domain K for the grasp map G is the direct sum of all the force domains of the contacting fingers [2].

(3) Other things being equal, when we choose a contact location we try to get away from the edge of the object because it is less "comfortable" there. Also in reality, all fingers have finite contact area and passive compliances. When such a finger is pressed against the object the fingertip tends to conform with the object. Under these conditions can the point contact model still predict accurately the force and velocity transformations? If we name the point where the object "matches" locally in shape with the fingertip a "regular point" and vice versa for a "irregular point" (Notice that a point on an edge will be therefore termed a very irregular point, and so on, see Appendix A for the exact definitions.) we will see that when a normal force is applied the contact pressure for an irregular point is much higher than for a regular point. Consequently, as was experimentally verified in [11] it will be much more difficult to transmit frictional forces through an irregular point than through a regular point. However, the point contact model developed with (G,K) does not distinguish between regular and irregular points. To have an accurate model and to enable an automatic grasp planner (see Section 3) get away from irregular points we need to incorporate the local contact geometry into the model. An apparent solution is to make K_i dependent on the local contact geometry in addition to the material properties of the

object. Thus, we assign to a "very regular" point the regular frictional cone and to a "very irregular" point a very thin frictional cone (i.e., with smaller friction coefficients). The technical details of this assignment are given in Appendix A. As the hardship in transmitting the frictional forces is reflected by the thin frictional cones we see that this modification of K_i captures the physical reality while still retaining the point contact model. In the sequel, the effective force domain K will mean one compensated with this procedure.

(4) The null space ($\eta(G)$) of the grasp map G is called the space of internal grasping forces [1, 4, 8]. Any applied finger forces in $\eta(G)$ do not contribute to the motion of the object. However, during the course of manipulation a set of nonzero internal grasping forces is needed to assure that the grasp is maintained. Usually, the set of desired internal grasping forces is higher for manipulation under an uncertain environment than for manipulation under a known environment. Both [1] & [8] have presented detailed discussions on the optimal choice of internal grasping forces.

We now proceed to develop the equations relating the joint velocities, torques to the body velocities, and wrenches: let the ith finger have m_i joints with joint variable denoted by $\theta_i = (\theta_{i1},...,\theta_{im_i})^t$. The forward kinematics of the finger manipulator relates the position and orientation of the ith finger coordinate frame C_{fi} by

$$g_{pf_i} : \mathrm{R}^{m_i} \to SE(3), \quad \text{with} \quad g_{pf_i} = \begin{bmatrix} A_{pf_i}(\theta_i) & r_{pf_i}(\theta_i) \\ 0 & 1 \end{bmatrix} \tag{2.2-5}$$

The generalized velocity $(v^s_{pf_i}, \omega^s_{pf_i})^t$ of the ith fingertip frame can be related to the $\dot{\theta}_i$ through the Jacobian of the forward kinematic equation (2.2-5) by

$$\begin{bmatrix} v_{pf_i} \\ \omega_{pf_i} \end{bmatrix} = \tilde{J}_i(\theta_i)\dot{\theta}_i \tag{2.2-6}$$

Here $\tilde{J}_i(\theta_i)$ is the Jacobian of the ith forward kinematic equation. Now the contact frame C_i and the fingertip frame C_{f_i} are located at the same point but may have different orientations. Consequently, the velocity of the ith fingertip frame C_{f_i} seen from the ith contact frame C_i using (2.1-13) with ($r_{if_i} = 0$) is given by

$$\begin{bmatrix} v_{p_i} \\ \omega_{p_i} \end{bmatrix} = \begin{bmatrix} A^s_{if_i} & 0 \\ 0 & A^s_{if_i} \end{bmatrix} \tilde{J}_i(\theta_i)\dot{\theta}_i \triangleq J_i(\theta_i)\dot{\theta}_i \tag{2.2-7}$$

In (2.2-7) above, A_{if_i} expresses the the relative orientation of the ith fingertip frame with respect to the ith contact frame and is given by $A_{if_i} = A_{bi}^{-1} \cdot A_{pb}^{-1} \cdot A_{pf_i}$. On the other hand, the motion $(v^s_{pb}, \omega^s_{pb})^t$ of the body as

seen from the ith contact frame is given by

$$\begin{bmatrix} v_{pi} \\ \omega_{pi} \end{bmatrix} = \begin{bmatrix} A_{bi}^t & -A_{bi}^t S(r_{bi}) \\ 0 & A_{bi}^t \end{bmatrix} \begin{bmatrix} v_{pb} \\ \omega_{pb} \end{bmatrix} \tag{2.2-8}$$

Now, the velocities as specified in (2.2-7) and (2.2-8) are not identical but agree along the directions specified by the basis matrix B_i. For example, for a point contact with friction, if the point of contact is not slipping then the translational velocities of the fingertips and the body coincide. For a soft finger contact with no slipping the translational velocity as well as the z-axis (in the contact frame) rotational velocity coincide. In contacts in which the fingertip rolls with respect to the surface of the body the constraints are more complicated [5, 27]. We take these constraints into account by insisting that

$$B_i^t J_i(\theta_i) = B_i^t T_{fi}^t \begin{bmatrix} v_{pb} \\ \omega_{pb} \end{bmatrix} \tag{2.2-9}$$

Concatenating equation (2.2-9) for $i = 1, \cdots, k$, and defining the hand Jacobian $J_h(\theta)$ by

$$J_h(\theta) = B^t J(\theta) \tag{2.2-10}$$

we obtain

$$J_h(\theta)\,\dot{\theta} = B^t J(\theta)\dot{\theta} = G^t \begin{bmatrix} v_{pb} \\ \omega_{pb} \end{bmatrix} \tag{2.2-11}$$

where

$$J(\theta) = \begin{bmatrix} J_1(\theta_1) & 0 & \cdots & 0 \\ 0 & J_2(\theta_2) & \cdots & \vdots \\ \vdots & \vdots & \cdots & \vdots \\ 0 & 0 & \cdots & J_k(\theta_k) \end{bmatrix}, \quad \theta = \begin{bmatrix} \theta_1 \\ \vdots \\ \theta_k \end{bmatrix} \tag{2.2-12}$$

and G^t is the transpose of the grasp map defined in (2.2-4).

Equation (2.2-11) is the equation relating the joint velocities to the generalized body velocity. The dual of equation (2.2-11) is an equation relating the joint torques of the fingers to the body wrench. We proceed to derive this now. Define $B_i\, x_i \in \mathrm{R}^6$ to be the finger wrench expressed in the ith contact frame with the $x_i \in \mathrm{R}^{m_i}$ representing the vector of applied finger wrenches. By the Principle of Virtual Work the resulting joint torque vector $\tau_i \in \mathrm{R}^{m_i}$ is related to $B_i x_i$ by

$$\tau_i = J_i^t(\theta_i) B_i x_i \tag{2.2-13}$$

Aggregating this equation for i=1,2, $\cdots k$ we get

$$\tau = J^t(\theta)Bx = J_h^t(\theta)\,x \quad \text{with } \tau \in \mathrm{R}^m,\ x \in \mathrm{R}^n,\ \textit{and}\ m = \sum_{i=1}^{k} m_i. \tag{2.2-14}$$

Also, as we have seen from the definition of the grasp map G in (2.2-4), that the body wrench (f_b, and m_b respectively) is given by

$$\begin{bmatrix} f_b \\ m_b \end{bmatrix} = Gx \tag{2.2-15}$$

We claim that the equations (2.2-14),(2.2-15) are a dual of the equation (2.2-11). To make the duality more explicit, we define

$$\lambda = G^t \begin{bmatrix} v_{pb} \\ \omega_{pb} \end{bmatrix}, \qquad \lambda \in \mathrm{R}^n \tag{2.2-16}$$

Then we may summarize the equations in the following table (see also Figure 4)

	Force Torque Relations	Velocity Relations
Body to Fingertip	$\begin{bmatrix} f_b \\ m_b \end{bmatrix} = Gx$	$\lambda = G^t \begin{bmatrix} v_{pb} \\ \omega_{pb} \end{bmatrix}$
Fingertip to Joints	$\tau = J_h^t(\theta)\,x$	$J_h(\theta)\dot{\theta} = \lambda$

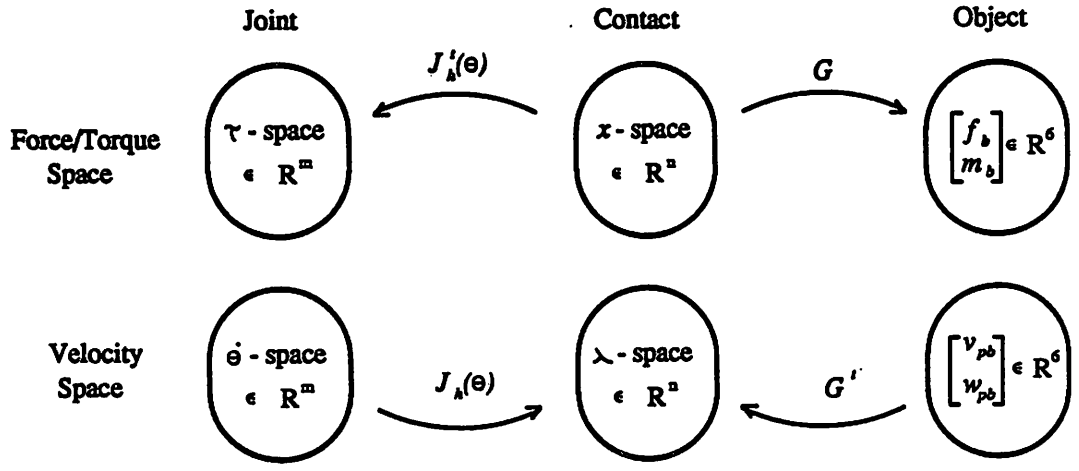

Figure 4. The force/torque and velocity transformation relations.

The following dual definitions are now intuitive.

Definition 2.3 (Stability and Manipulability of a Grasp) *Consider a grasp by a multifingered hand with k fingers each having m_i joints, $i=1,\cdots k$ and with fingertips having contacts with n_i degrees of freedom, $i=1,\cdots k$. Let $\theta \in R^m, \tau \in R^m$ represent the joint angles and torques respectively. Then:*

(i) The grasp is said to be stable if, for every wrench $(f_b^t, m_b^t)^t$ applied to the body, there exists a choice of joint torque τ to balance it.

(ii) The grasp is said to be manipulable if, for every motion of the body, specified by $(v_{pb}^t, \omega_{pb}^t)^t$, there exists a choice of joint velocity $\dot{\theta}$ to impart this motion without breaking contact.

Grasp stability and manipulability are now easily characterized for a given position of the fingers by

Proposition 2.4: *(i) A grasp is stable if and only if G is onto, i.e. the range space of G is the entire R^6. (ii) A grasp is manipulable if and only if $R(J_h(\theta)) \supset R(G^t)$, where $R(\cdot)$ denotes the range space of.*

Remark: The conditions (i) and (ii) superficially appear to be distinct, but they are related. Let us begin by examining the implications of condition (i) on grasp manipulability.

Consider Figure 4 focusing attention especially on the two orthogonal direct sum decompositions of R^n given by

$$R^n = R(G^t) \oplus \eta(G) \tag{2.2-17}$$

$$= R(J_h(\theta) \oplus \eta(J_h^t(\theta))$$

If G is onto, then equation (2.2-15) has a solution. Furthermore, the solution will be unique in the range space of G^t (the least norm solution of (2.2-15)). If for some body wrench there exists an x that needs zero joint torque, then $R(G^t) \cap \eta(J_h^t(\theta)) \neq \phi$ and consequently the condition $R(J_h(\theta)) \supset R(G^t)$ fails. This implies that the grasp is not manipulable.

For the converse, consider the implication of condition (ii) on grasp stability. Suppose that $R(J_h) \supset R(G^t)$ and there exists a body velocity (v_{pb}, ω_{pb}) which produces zero λ and consequently zero $\dot{\theta}$, then $\eta(G^t) \neq \phi$ and therefore G can not be onto. This implies that the grasp is not stable.

To give simple examples to illustrate the foregoing comments, it is of interest to specialize the definitions to the plane. For grasping in the $x-y$ plane, the only forces and torques that need to be considered are $(f_x, f_y, m_z)^t \in R^3$ and the velocities $(v_x, v_y, \omega_z)^t \in R^3$. Figure 5 now shows a planar two fingered grasp which is stable but not manipulable. The two fingers are one jointed and the contacts are point contacts with friction. A force f_y can be resisted with no joint torque τ_1, τ_2. However the grasp is not manipulable, since a y-direction velocity on the body cannot be accommodated.

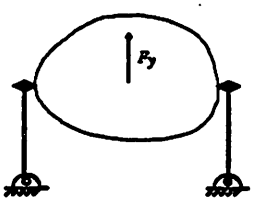

Figure 5: A stable but not manipulable grasp

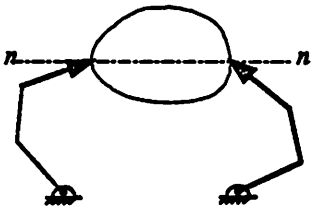

Figure 6: A manipulable but not stable grasp

Figure 6 shows a grasp of a body in R^3 by two three jointed fingers. The contacts are point contacts with friction. The grasp is manipulable, since $J_h(\theta)$ has rank 6, though the object can spin around the axis $n-n$ with zero joint velocities $\dot{\theta}$. However the grasp is not stable since a body torque τ_n about the axis $n-n$ cannot be resisted by any combination of joint torques.

In view of the preceeding discussion, we will require the grasp to be both manipulable and stable, i.e.,

$$R(G) = R^6 \quad \text{and} \quad R(J_h(\theta)) \supset R(G^t) \tag{2.2-18}$$

Condition (i) suffers from the drawback that the force domain is left completely unconstrained. As we have seen earlier the forces are constrained to lie in a convex cone K, taking into account the unidirectionality of the contact forces, finite friction, etc, in which case the image of $K \cap R(J_h)$ under G should cover all of R^6. If we generalize the previous definitions to formally define a grasp to be $\Omega = (G, K, J_h(\theta))$ we have the modified stability and manipulability conditions of a grasp by

Corollary 2-5: *A grasp under unisense and finite frictional forces is both stable and manipulable if and only if*

$$G(K \cap R(J_h)) = R^6, \text{ and } R(J_h) \supset R(G^t) \tag{2.2-19}$$

3. Grasp Planning

Typical tasks associated with multifingered robot hands include scribing, inserting a peg into a hole, assembly operations. Common to these tasks are the fact that the robot hand must manipulate an object from one configuration to another, while exerting a set of desired contact forces on the environment. Successful execution of such tasks amounts to having the robot hand perform a sequence of operations: (1) selecting a "good" grasp on the object, and (2) using the cooperative action of the fingers to control the object. As we can see that the first operation is essential to the execution of the task. For example, if a pencil is not grasped at the right position and with the right postures of the fingers, it will be extremely difficult to perform a scribing task. In this section we study how to generate a "good" grasp for a given task and in the next section we study how to manipulate the object with the cooperative action of the fingers.

The term "a good grasp" is not well defined unless a criterion for evaluating a grasp is given. In the literature various stability criteria used to characterized a grasp have been proposed and studied extensively [3, 10, 13]. But, in many cases such a criterion is too rough as it may generate a large number of stable grasps to a given object. For example, for a pencil there exist infinitely many choices of stable grasps, and while some are satisfactory for the scribing task some others are not. To solve this problem, additional criteria have been proposed in [2] & [17], for example the minimum singular value of the grasp matrix G, the determinant of GG^t [2], and some objective functions defined in [17].

After investigating human grasps, the author in [6] has suggested using the task requirement as the criterion for evaluating a grasp. Several other researchers also have had studies in incorporating the task requirement into the selection of a grasp. In [3, 15] a task is modeled by a desired compliance matrix and the final grasp is then required to have the desired compliance property. In [16] a task is modeled by a desired inertia matrix about some operating point, and the final grasp is required to have the desired inertia property at the operating point. In [2] a task is modeled by an ellipsoid, called the task ellipsoid, in the wrench space of the object, and the final grasp is required to maximize the task ellipsoid with unit control effort. While all the above three approaches were concerned with the selection of a task oriented optimal grasp, the nature of the tasks addressed among them are different. In [3, 15] the tasks are quasi static and the system potential energy is assumed to dominate the kinetic energy. In [16] the tasks are purely dynamic and the inertia property rather than the compliance property is the main concern in the grasp selection process. On the other hand, the approach via [2] does apply to both classes of tasks, but it lacks the level of generality in the sense that only the wrench space and the grasp map G were considered in the optimization process.

In this section, we extend the work of [2] to consider in the selection process the aggregated behavior of $\Omega = (G, K, J_h)$ in both the wrench space and the twist space. Task modeling by task ellipsoids will take place in both the wrench space and the twist space. As in [2] the methodology of modeling a task is to associate each task one ellipsoid (A_α) in the wrench space and another ellipsoid (B_β) in the twist space. The shape of the ellipsoid A_α (B_β respectively) reflects the relative force requirement (or the motion requirement) of the task. For example, if the relative force requirement in a certain direction, such as the normal direction of the grinding application with a grinding tool, is high the task ellipsoid A_α then is shaped long in that direction. To demonstrate the precise implications of the methodology we study task modeling for the following two tasks.

Example 3-1: Consider the peg insertion task depicted in Figure 7 where the robot grasps the workpiece and inserts it into the hole.

In order to execute the task, a nominal trajectory is planned before grasping. After grasping the hand follows the planned trajectory until some misalignment of the peg causes the object to deviate from the nominal trajectory and collide with the environment.

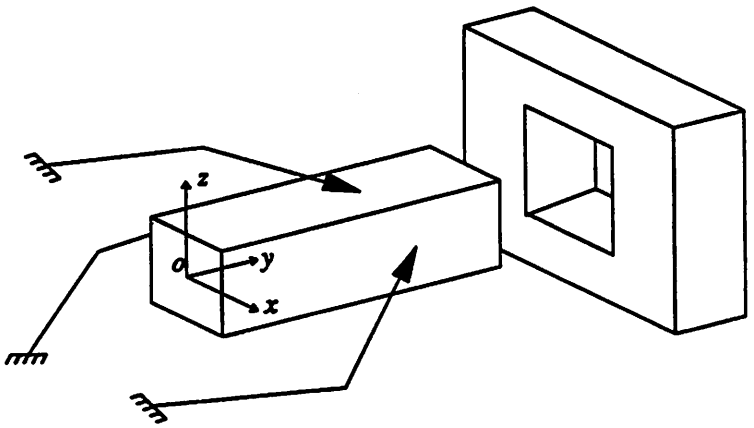

Figure 7: Peg-in-hole task

With the body coordinate chosen as shown, the likehood of collision forces in each force direction of decreasing order would be $-f_y$, $\pm\tau_z$, $\pm\tau_x$, $\pm f_z$, $\pm f_x$, $\pm\tau_y$ and $+f_y$. If we denote by $(r_i)_{i=1}^6$ the ratio of maximum expected collision forces in each direction, we obtain a set A_α, parametrized by $\alpha \in [0, \infty)$, in the wrench space space of the object by

$$A_\alpha = \left\{ (f_x, \cdots \tau_z) \in R^6, \frac{(f_y + c_1)^2}{r_1^2} + \frac{\tau_z^2}{r_2^2} + \frac{\tau_x^2}{r_3^2} + \frac{(f_z - c_2)^2}{r_4^2} + \frac{f_x^2}{r_5^2} + \frac{\tau_y^2}{r_6^2} \le \alpha^2 \right\} \quad (3.0\text{-}1a)$$

where the constant c_1 reflects the offset of maximum expected collision force between $+f_y$ and $-f_y$

directions, and c_2 reflects the gravitational force on the object. The set A_α is an ellipsoid in the wrench space centered at $(0, c_1, c_2, 0, 0, 0)$, with the principal axes given by the generalized force directions, and axes lengths by the corresponding ratios r_i. The size of the ellipsoid is scaled by the parameter α.

By appropriately assigning a set of values to the constants (r_i, i=1, ... 6) and (c_i, i=1, 2) we can decide on the shape of the ellipsoid so that it reflects the task requirement in the wrench space. In particular, the peg insertion task requires that ($r_i \geq r_j$) whenever $i \geq j$ and c_1 to be large when collision forces in $+f_y$ direction are very unlikely.

On the other hand, since the peg insertion task requires precise positioning the grasp should provide good manipulation capability (or dexterity) in certain directions. First, in the v_y direction relatively large motion is needed. Then, the grasp should be very sensitive in ω_y, v_z and v_x directions. If we model by $(\delta_i)_{i=1}^6$ the ratio of relative maximum motion requirement among the six generalized velocity directions we obtain an ellipsoid B_β in the twist space, parametrized by $\beta \in [0, \infty)$, define by

$$B_\beta = \left\{ (v_x, \cdots, \omega_z) \in R^6, \frac{v_x^2}{\delta_1^2} + \frac{v_y^2}{\delta_2^2} + \frac{v_z^2}{\delta_3^3} + \frac{\omega_x^2}{\delta_4^2} + \frac{\omega_y^2}{\delta_5^2} + \frac{\omega_z^2}{\delta_6^2} \leq \beta^2 \right\} \qquad (3.0\text{-}1b)$$

The shape of B_β reflects the task requirement in the twist space. In this case δ_2, δ_3 and δ_4 are relatively larger than the other constants. Precise values of these constants can be obtained from experiments or experience through error-and-trial procedures.

Example 3-3: Consider the task of scribing with a pencil. Human experience tells us that, in order to execute the task efficiently, the grasp should provide, (1) good dexterity at the lead and (2) sufficient normal forces. With the body coordinate shown in the figure, the task requirement can be translated into requirements on the two task ellipsoids by (a) the task ellipsoid B_β in the twist space should be long in ω_y and ω_z directions and flat in the other directions, and (b) the task ellipsoid A_α in the wrench space should be long in f_x direction and then τ_z and τ_y directions. Applying this reasoning we obtain in (3.0-2) two task ellipsoids A_α and B_β that describe the relative force and velocity ratios of the task.

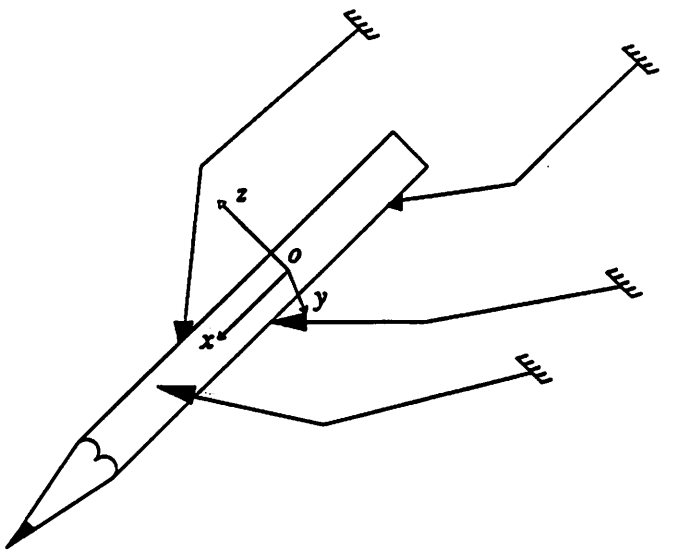

Figure 8. A scribing task.

$$A_\alpha=\left\{ (f_x, \cdots, \tau_z) \in R^6, \frac{(f_x+c)^2}{r_1^2}+\frac{f_y^2}{r_2^2}+\frac{f_z^2}{r_3^2}+\frac{\tau_x^2}{r_4^2}+\frac{\tau_y^2}{r_5^2}+\frac{\tau_z^2}{r_6^2} \le \alpha^2 \right\} \qquad (3.0\text{-}2a)$$

Wrench Space Task Ellipsoid

$$B_\beta=\left\{ (v_x, \cdots, \omega_z) \in R^6, \frac{v_x^2}{\delta_1^2}+\frac{v_y^2}{\delta_2^2}+\frac{v_z^2}{\delta_3^2}+\frac{\omega_x^2}{\delta_4^2}+\frac{\omega_y^2}{\delta_5^2}+\frac{\omega_z^2}{\delta_6^2} \le \beta^2 \right\} \qquad (3.0\text{-}2b)$$

Twist Space Task Ellipsoid

To conclude these examples, we emphasize that to each task we can associate two task ellipsoids, one in the wrench space that represents the relative force requirement and the other in the twist space that represents the relative motion requirement of the task. The constants (r_i, δ_i, c_i) that determine shapes of these ellipsoids can be obtained from experiments or from experience with similar tasks. Hence, we need to store in a library a set of ellipsoid data for a set of interesting tasks, which usually involves considerable modeling effort. In the sequel, A_α will denote a task ellipsoid in the wrench space and B_β one in the twist space.

3.1. The Task Oriented Quality Measures for Grasp Planning

We have shown that a grasp $\Omega = (G, K, J_h)$ contains information about the locations of the fingertips on the object (G and K) and the postures of the fingers (J_h). Also, we have modeled a particular task by two ellipsoids A_α and B_β. We now integrate these to develop two quality measures for a grasp, one in the twist space and the other in the wrench space.

Definition 3-5 (The Twist Space Quality Measure μ_t): *Following the previous notation we let $O_1^m \subset R^m$ denote the unit ball in R^m, the space of finger joint velocities, and define the task oriented twist space quality measure $\mu_t(\Omega)$ of a grasp Ω by*

$$\mu_t(\Omega) = \sup_{\beta \in R_+} \{ \beta, \text{ such that } J_h(O_1^m) \supset G^t(B_\beta) \} \tag{3.1-1}$$

The geometric meaning of $\mu_t(\Omega)$ is as follows(see Figure 9): the unit ball O_1^m in the finger joint velocity space is mapped into the space of fingertip velocity by J_h. On the other hand, a task ellipsoid B_β in the twist space is mapped back into the fingertip velocity space by G^t; $\mu_t(\Omega)$ is then the radius β of the largest task ball B_β such that $G^t(B_\beta)$ is *contained* in $J_h(O_1^m)$. From a theoretical point of view, $\mu_t(\Omega)$ is the ratio of the *"structured" output (i.e., the task ellipsoid)* over the input (i.e., the finger joint velocity). We also see from the figure that $\mu_t(\Omega)$ is at its maximum if the inner ellipsoid has the same shape and orientation as the outer ellipsoid.

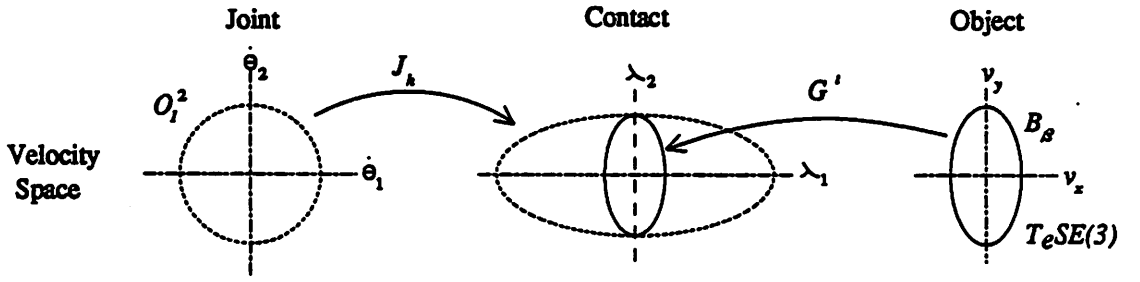

Figure 9

Definition 3-6 (The Wrench Space Quality Measure μ_w): *We define the wrench space task oriented quality measure μ_w of Ω by the following procedure:*

(a) Define $A_1 \subset R^6$ to be the unit task ellipsoid in the wrench space, and O_γ^n the ball of radius γ, $\gamma \in [0, \infty)$, in the finger wrench space;

(b) Define $\alpha = \inf_{\gamma \in R_+} \{\gamma,$ such that $G(O_\gamma^n \cap K \cap R(J_h)) \supset A_1\}$. Thus, O_α^n is the smallest ball in the finger wrench space that will cover the unit task ellipsoid.

(c) Define $C(\alpha) = J_h^t(O_\alpha \cap K \cap R(J_h))$ to be the corresponding set in the finger joint torque space, it is the set of joint torques that will cover the unit task ellipsoid.

(d) We define the worst case cost function of the input set $C(\alpha)$ by

$$\text{Cost}(C(\alpha)) = \sup_{y \in C(\alpha)} \| y \| \tag{3.1-2}$$

where $\| y \|$ stands for the magnitude of the vector y, and the wrench space quality measure $\mu_w(\Omega)$ by

$$\mu_w(\Omega) = \frac{1}{Cost(C(\alpha))} \tag{3.1-3}$$

Remark: We interpret the geometric meaning of the above steps as follows (see Figure 10): (1) in steps (a) and (b) we find the smallest ball in the finger wrench space that will cover the unit task ellipsoid through the transformation G; (2) such a ball is mapped back into the joint torque space and its cost function is defined by (3.1-2), which is the distance of the furtherest point in the set from the origin. (3) The quality measure is then the inverse of this cost (Notice that one may also use the quadratic cost function, or any other cost functions in (3.1-2)).

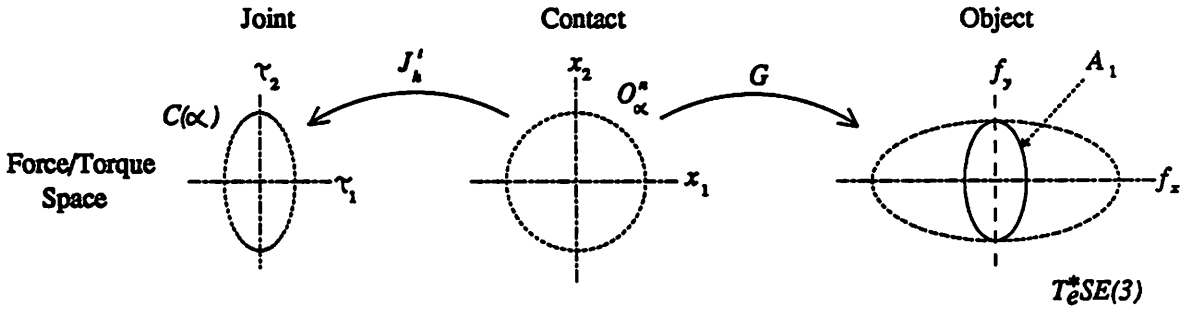

Figure 10

These quality measures defined in Definition 3-5 and 3-6 provide useful characterization of a grasp, but are difficult to compute (see for e.g. [2]). However, when the task ellipsoids are specialized to the unit balls in their respective spaces and K is R^n itself we do have the following results:

Proposition 3-7: *Under the condition that $K = R^n$, A_1 and B_1 are unit balls in R^6 the quality measures defined in Definition 3-5 and 3-6 are given by*

$$\mu_t(\Omega) = \frac{\sigma_{min}(J_h)}{\sigma_{max}(G^t)} = \frac{\sigma_{min}(J_h)}{\sigma_{max}(G)} \tag{3.1-4}$$

and

$$\mu_w(\Omega) = \frac{\sigma_{min}(G)}{\sigma_{max}(J_h^t)} = \frac{\sigma_{min}(G)}{\sigma_{max}(J_h)} \tag{3.1-5}$$

where σ_{min}, σ_{max} are the minimum, maximum singular values respectively.

The proof follows from applying the definition of the singular value decomposition of a matrix to Definition 3-5 and 3-6 respectively.

Remark: The quality measures defined here are called the min-max type of measures [2]. In the special case of a single manipulator, G is the identity matrix and the two quality measures (3.1-4) and (3.1-5) are just $\sigma_{min}(J_h)$ and $\sigma_{max}^{-1}(J_h)$ respectively. To generalize the volume measures defined in

[2, 9, & 12] to a multifingered hand, we first assume that the grasp is both stable and manipulable, i.e., Proposition 2-4 holds, and denote the singular values of G by $(\delta_1 \geq \delta_2 \geq \cdots \geq \delta_6 > 0)$, and the singular values of J_h by $(\sigma_1 \geq \sigma_2 \geq \cdots \geq \sigma_n > 0)$. Then, the corresponding manipulability and stability volume measures of a grasp can be defined as

$$\mu_t(\Omega) = \frac{(\delta_1 \cdot \cdots \cdot \delta_6)}{(\sigma_1 \cdot \cdots \cdot \sigma_n)} = \frac{\det(G\, G^t)}{\det(J_h\, J_h^t)} \tag{3.1-4b}$$

and

$$\mu_w(\Omega) = \frac{(\sigma_1 \cdot \cdots \cdot \sigma_n)}{(\delta_1 \cdot \cdots \cdot \delta_6)} = \frac{\det(J_h\, J_h^t)}{\det(G\, G^t)} \tag{3.1-5b}$$

The quality measures given by (3.1-4) and (3.1-5) can be easily computed using the singular value decomposition data of G and J_h. A grasp Ω_1 is said to be a better grasp than another grasp Ω_2 if Ω_1 has higher quality measures in both spaces than Ω_2, and a "good grasp" is defined to have high quality measures in both spaces. Notice that the definitions (3.1-4) and (3.1-5) exhibit an interesting dual relationship in the following sense (see also Section 2.2): $\mu_t(\Omega)$ increases if $\sigma_{min}(J_h)$ increases or if $\sigma_{max}(G)$ decreases, and $\mu_w(\Omega)$ increases if $\sigma_{max}(J_h)$ decreases or if $\sigma_{min}(G)$ increases. Thus, we can simultaneously increase both quality measures only to a certain point and then the quality measure in one space decreases as the quality measure in the other space increases. We propose the following procedure for grasp planning:

(1) Define the performance measure (PM) of a grasp Ω by

$$PM = \gamma\, \mu_t(\Omega) + (1-\gamma)\mu_w(\Omega) \tag{3.1-6}$$

where $\gamma \in [0, 1]$ is called the relative importance ratio between the manipulability measure and the stability measure. $\gamma > 0.5$ indicates that the task is motion oriented and $\gamma < 0.5$ indicates that the task is stability oriented. We suggest further studies on determining the relation of γ with the task nature.

(2) Use the performance measure, geometry of the object and structures of the hand to formulate the corresponding optimization problem (see [2] for details).

(3) Solve the optimization problem to find the Ω that maximizes the performance measure.

Example 3-8: Consider the two-fingered planar manipulation system shown in Figure 12. We model the contact to be a point contact with friction, and choose the following values for the system parameters:

Finger manipulator spacing $r = 1$;

Finger manipulator link length $l_1 = l_2 = 1$.

At the grasping location shown in the figure, the grasp map G is

$$G = \begin{bmatrix} -1 & 0 & 1 & 0 \\ 0 & -1 & 0 & 1 \\ 0 & -r & 0 & -r \end{bmatrix} \tag{3.1-7}$$

and the hand Jacobian J_h is

$$J_h = \begin{bmatrix} J_1 & 0 \\ 0 & J_2 \end{bmatrix} \tag{3.1-8}$$

where

$$J_1 = \begin{bmatrix} \cos\alpha & -\sin\alpha \\ \sin\alpha & \cos\alpha \end{bmatrix} \begin{bmatrix} -\sin\theta_{11} - \sin(\theta_{11}+\theta_{12}) & -\sin(\theta_{11}+\theta_{12}) \\ \cos\theta_{11} + \cos(\theta_{11}+\theta_{12}) & \cos(\theta_{11}+\theta_{12}) \end{bmatrix} \tag{3.1-9}$$

and

$$J_2 = \begin{bmatrix} -\cos\alpha & \sin\alpha \\ -\sin\alpha & -\cos\alpha \end{bmatrix} \begin{bmatrix} -\sin\theta_{21} - \sin(\theta_{21}-\theta_{22}) & \sin(\theta_{21}-\theta_{22}) \\ \cos\theta_{21} + \cos(\theta_{21}-\theta_{22}) & -\cos(\theta_{21}+\theta_{22}) \end{bmatrix} \tag{3.1-10}$$

Subject to the kinematic constraint (2.2-9) the system has three degree of freedoms. If we further constrain the system so that the object moves vertically and with constant orientation angle $\alpha = 0$ the system has a single degree of freedom. Let us choose θ_{11} to be the generalized coordinate of the system and study the simplified optimization problem, where the quality measures (3.1-4), (3.1-5) and the performance measure are maximized by varying θ_{11}. Figure 11 shows plots of the quality measures and the performance measure as functions of θ_{11}. We see that the manipulability measure μ_t is at its maximum when θ_{11} is about 30^o (= 0.52 radian), which corresponds to the grasping configuration with $\theta_{12} = 120^o$, $\theta_{21} = 150^0$ and $\theta_{22} = 120^o$. The stability measure decreases monotonically as θ_{11} is increased. However, the performance measure with $\gamma = 0.5$ and $\gamma = 0.75$ reaches its maximum at $\theta_{11} = 18^o$ ($\theta_{12} = 144^o$, $\theta_{21} = 162^o$ and $\theta_{22} = 144^o$), and at $\theta_{11} = 24^o$ ($\theta_{12} = 132^o$, $\theta_{21} = 156^o$ and $\theta_{22} = 132^o$) respectively. The grasp has zero manipulability measure both at $\theta_{11} = 90^o$ and at $\theta_{11} = 0^o$, where the first case corresponds to Figure 5. The optimal value of θ_{11} for the performance measure goes up when more weight is given to the manipulability measure. Thus, we see that the parameter γ is an important factor in grasp planning.

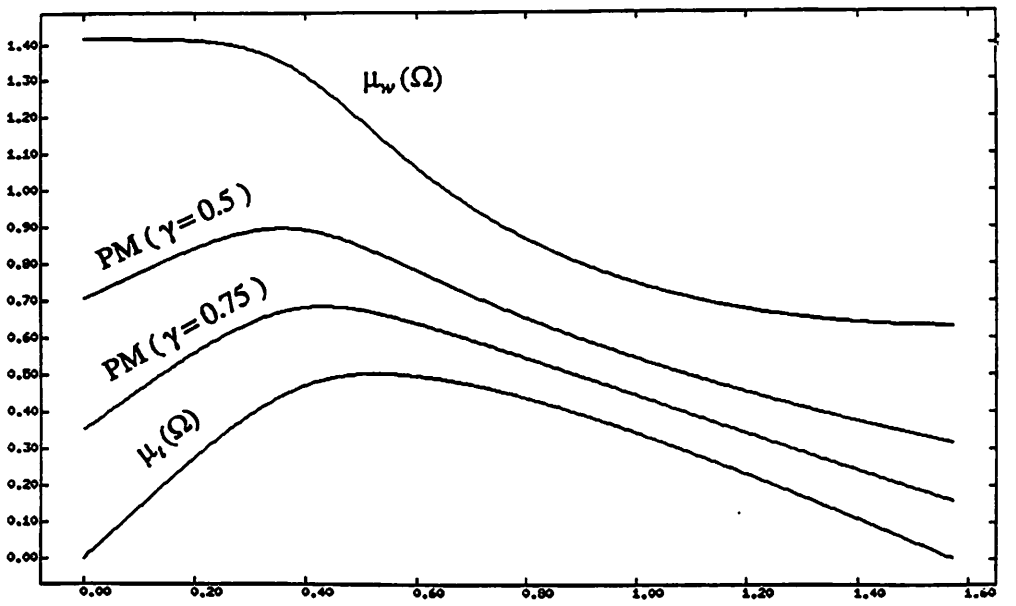

Figure 11. Quality measures and performance index versus θ_{11}.

4. Coordinated Control of a Multifingered Hand

In this section, we develop control algorithms for the coordinated control of a multifingered robot hand. The goal of the control scheme is to specify a set of control inputs for the finger motors so that the gripped object undergoes a desired body motion while exerting a set of desired contact forces on the environment.

Previous researchers have suggested the so-called "master-slave" control methodology for two robot manipulators (see, for e.g. [23, 24]). Others have generalized this method to a group of several manipulators (or a multifingered robot hand) [25]. In [26] an alternative approach was proposed. But it assumed rigid attachment of the fingertip to the object and each finger manipulator needed to be six jointed.

We present a generalization of the computed torque methodology as our methodology for the control of a group of manipulators. Without loss of generality, we may assume that the desired task is: (1) to manipulate the object along the following prespecified trajectory

$$g_{pb,d}(t) = \begin{bmatrix} A_{pb,d}(t) & r_{pb,d}(t) \\ 0 & 1 \end{bmatrix} \in SO(3)\times R^3 \tag{4.0-1}$$

and (2) to maintain a set of desired internal grasping forces during the course of manipulation. We make the following assumption about the grasp:

(A1): The grasp is both stable and manipulable (see Corollary 2-6).

A necessary condition for (A1) to hold is that both the grasp map G and the hand Jacobian $J_h(\theta) = B^t J(\theta)$ be of full rank. From Section 2.2, we know that in order to maintain the contact during manipulation the finger joint velocity $\dot{\theta}$ and the object velocity $[v_{pb}^t, \omega_{pb}^t]^t$ must satisfy the following velocity constraint relation:

$$J_h(\theta)\dot{\theta} = G^t \begin{bmatrix} v_{pb} \\ \omega_{pb} \end{bmatrix} \tag{4.0-2}$$

Differentiating (4.0-2), we obtain the following acceleration constraint equation

$$J_h(\theta)\ddot{\theta} + \dot{J}_h(\theta)\dot{\theta} = G^t \begin{bmatrix} \dot{v}_{pb} \\ \dot{\omega}_{pb} \end{bmatrix} \tag{4.0-3}$$

Since $R(J_h(\theta)) \supset R(G^t)$ by assumption (A1), we may express the joint acceleration $\ddot{\theta}$ in terms of the object acceleration $[\dot{v}_{pb}^t, \dot{\omega}_{pb}^t]^t$ by

$$\ddot{\theta} = J_h^+ G^t \begin{bmatrix} \dot{v}_{pb} \\ \dot{\omega}_{pb} \end{bmatrix} - J_h^+ \dot{J}_h \dot{\theta} + \ddot{\theta}_o \tag{4.0-4}$$

here $J_j^+ = J_h^t(J_h J_h^t)^{-1}$ is the generalied inverse of J_h, and $\ddot{\theta}_o \in \eta(J_h)$ is the internal motion of redundant joints not affecting the object motion.

Remark: (1) Using (4.0-4) we can develop the control algorithm in the operational space of the body being manipulated. But if we express the object acceleration in terms of $\ddot{\theta}$ by

$$[v_{pb}^t, \omega_{pb}^t]^t = (GG^t)^{-1}(J_h \ddot{\theta} + \dot{J}_h \dot{\theta})$$

we can develop a control algorithm in the joint space of the fingers. In future work we will consider this alternative since it appears to hold some interesting and different possibilities.

(2) When J_h is square, its generalized inverse J_h^+ is just the usual inverse, and $\ddot{\theta}_o$ disappears from (4.0-4). This also implies that the joint motion is determined uniquely by the motion of the object.

The dynamics of the object are given by the Newton-Euler equations

$$\begin{bmatrix} m & 0 \\ 0 & I \end{bmatrix} \begin{bmatrix} \dot{v}_{pb} \\ \dot{\omega}_{pb} \end{bmatrix} + \begin{bmatrix} \omega_{pb} \times m v_{pb} \\ \omega_{pb} \times I \omega_{pb} \end{bmatrix} = \begin{bmatrix} f_b \\ m_b \end{bmatrix} \tag{4.0-5}$$

where $m \in R^{3\times3}$ is the diagonal matrix with the object mass in the diagonal, $I \in R^{3\times3}$ is the object inertia matrix with respect to the body coordinates, and $[f_b^t, m_b^t]^t$ is the applied body wrench in the body coordinates which is also related to the applied finger wrench $x \in R^n$ through

$$Gx = \begin{bmatrix} f_b \\ m_b \end{bmatrix} \tag{4.0-6}$$

Since we have assumed that the grasp is stable, i.e., G is onto, we may solve (4.0-6) as

$$x = G^+ \begin{bmatrix} f_b \\ m_b \end{bmatrix} + x_o \tag{4.0-7}$$

where $G^+ = G^t(GG^t)^{-1}$ is the left inverse of G, and $x_o \in \eta(G)$ is the internal grasping force. Part of the control objective is to steer the internal grasping force x_o to a certain desired value $x_{o,d} \in \eta(G)$.

Combining (4.0-5) and (4.0-7) yields

$$x = G^+ \left\{ \begin{bmatrix} m & 0 \\ 0 & I \end{bmatrix} \begin{bmatrix} \dot{v}_{pb} \\ \dot{\omega}_{pb} \end{bmatrix} + \begin{bmatrix} \omega_{pb} \times m v_{pb} \\ \omega_{pb} \times I \omega_{pb} \end{bmatrix} \right\} + x_o \tag{4.0-8}$$

4.1. The Control Algorithm

The dynamics of the i th finger manipulator is given by

$$M_i(\theta_i)\ddot{\theta}_i + N_i(\theta_i,\dot{\theta}_i) = \tau_i - J_i^t(\theta_i)B_i x_i \tag{4.1-1}$$

Here, as is common in the literature $M_i(\theta_i)\in R^{n_i \times n_i}$ is the moment of inertia matrix of the i th finger manipulator, $N_i(\theta_i,\dot{\theta}_i)\in R^{n_i}$ the centrifugal, Coriolis and gravitational force terms, τ_i the vector of joint torque inputs and $B_i x_i \in R^6$ the vector of applied finger wrenches. Define

$$M(\theta) = \begin{bmatrix} M_1(\theta_1) & 0 & \cdots & 0 \\ 0 & M_2(\theta_2) & \cdots & \vdots \\ \vdots & \vdots & \ddots & \vdots \\ 0 & 0 & \cdots & M_k(\theta_k) \end{bmatrix}, \quad N(\theta,\dot{\theta}) = \begin{bmatrix} N_1(\theta_1,\dot{\theta}_1) \\ \vdots \\ N_k(\theta_k,\dot{\theta}_k) \end{bmatrix} \quad \text{and} \quad \tau = \begin{bmatrix} \tau_1 \\ \vdots \\ \tau_k \end{bmatrix} \tag{4.1-2}$$

Then, the finger dynamics can be grouped to yield

$$M(\theta)\ddot{\theta} + N(\theta,\dot{\theta}) = \tau - J_h(\theta)^t x \tag{4.1-3}$$

The control objective is to specify a set of joint torque inputs τ so that both the desired body motion $g_{ro,d}(t)$ and the desired internal grasping force x_{od} are realized.

Since SO(3) is a compact three dimensional manifold, we may locally parametrize it by either the Euler angles, the Pitch-roll-yaw variables [20,22], or the exponential coordinates ([22]). Let $\phi_{pb} = [\phi_1,\phi_2,\phi_3]^t$ be a parametrization of SO(3), we can express the body trajectory $g_{pb}(t)$ as

$$g_{pb}(t) = \begin{bmatrix} A_{pb}(\phi_{pb}(t)) & r_{pb}(t) \\ 0 & 1 \end{bmatrix} \in \text{SO(3)}\times R^3 \tag{4.1-4}$$

and the body velocity as

$$\begin{bmatrix} v_{pb}(t) \\ \omega_{pd}(t) \end{bmatrix} = U(\phi_{pb}(t),r_{pb}(t)) \begin{bmatrix} \dot{r}_{pb}(t) \\ \dot{\phi}_{pb}(t) \end{bmatrix} \tag{4.1-5}$$

where $U(\phi_{pb}(t),r_{pb}(t))\in R^{6\times 6}$ is a parametrization dependent matrix that relates the derivatives of the parameterization to the body velocity. Differentiating (4.1-5) yields

$$\begin{bmatrix} \dot{v}_{pb}(t) \\ \omega_{pb}(t) \end{bmatrix} = U \begin{bmatrix} \ddot{r}_{pb}(t) \\ \ddot{\phi}_{pb}(t) \end{bmatrix} + \dot{U} \begin{bmatrix} \dot{r}_{pb}(t) \\ \dot{\phi}_{pb}(t) \end{bmatrix} \tag{4.1-6}$$

Theorem 4-1: *Assume that (A1) holds and that the fingers are nonredundant, i.e., $m_i = n_i$, for $i = 1,\cdots k$. Define the position error $e_p\in R^6$ to be*

$$e_p = \begin{bmatrix} r_{pb} \\ \phi_{pb} \end{bmatrix} - \begin{bmatrix} r_{pb,d} \\ \phi_{pb,d} \end{bmatrix} \tag{4.1-7}$$

where $[r_{pb,d}, \phi_{pb,d}]$ is the desired body trajectory, and the internal grasping force error $e_f \in R^{n-6}$ to be

$$e_f = x_o - x_{o,d} \tag{4.1-8}$$

where $x_{o,d}$ is the desired internal grasping force. Then, the control law specified by (4.1-9) realizes not only the desired body trajectory but also the desired internal grasping force.

$$\tau = N(\theta,\dot{\theta}) + J_h^t G^+ \begin{bmatrix} \omega_{pb} \times m v_{pb} \\ \omega_{pb} \times I\,\omega_{pb} \end{bmatrix} - M(\theta) J_h^{-1} \dot{J}_h \dot{\theta} + M_h \dot{U} \begin{bmatrix} \dot{r}_{pb} \\ \dot{\phi}_{pb} \end{bmatrix} \tag{4.1-9a}$$

$$+ J_h^t (x_{o,d} - K_I \int e_f) + M_h U \left\{ \begin{bmatrix} \ddot{r}_{pb,d} \\ \dot{\phi}_{pb,d} \end{bmatrix} - K_v \dot{e}_p - K_p e_p \right\}$$

where

$$M_h = M(\theta) J_h^{-1} G^t + J_h^t G^+ \begin{bmatrix} m & 0 \\ 0 & I \end{bmatrix} \tag{4.1-9b}$$

and K_I is a martix that maps any vector in the null space of G into the null space of G.

Remarks: (1). (4.1-9) can be generalized to the redundant case and the results are given in Appendix B.

(2) The first four components in (4.1-9a) are used for cancellation of Coriolis, gravitational and centrifugal forces. These terms behave exactly like the nonlinearity cancellation terms in the computed torque control for a single manipulator; the term $J_h^t(x_{o,d} - K_I \int e_f)$ is the compensation for the internal grasping force loop, and the last term is the compensation for the position loop. We will see in the proof that the dynamics of the internal grasping force loop and that of the position loop are mutually decoupled. Consequently, we can design the force error integral gain K_I independently from the position feedback gains K_v and K_p.

Proof:

The proof is very procedural and straightforward. First, we substitute (4.0-4) and (4.0-8) into (4.1-3) to get

$$M(\theta)\left\{ J_h^{-1} G^t \begin{bmatrix} \dot{v}_{pb} \\ \dot{\omega}_{pb} \end{bmatrix} - J_h^{-1} \dot{J}_h \dot{\theta} \right\} + N(\theta,\dot{\theta}) = \tau - J_h^t \left\{ G^+ \begin{bmatrix} m & 0 \\ 0 & I \end{bmatrix} \begin{bmatrix} \dot{v}_{pb} \\ \dot{\omega}_{pb} \end{bmatrix} + G^+ \begin{bmatrix} \omega_{pb} \times m v_{pb} \\ \omega_{pb} \times I\,\omega_{pb} \end{bmatrix} \right\} - J_h^t x_o \tag{4.1-10}$$

Note that in (4.0-4) the generalized inverse for non-redundant fingers reduces to the regular inverse J_h^{-1} and $\ddot{\theta}_o = 0$. If we choose the following control in (4.1-10)

$$\tau = N(\theta,\dot{\theta}) + J_h^t G^t \begin{bmatrix} \omega_{pb} \times m v_{pb} \\ \omega_{pb} \times I\,\omega_{pb} \end{bmatrix} - M(\theta) J_h^{-1} \dot{J}_h \dot{\theta} + \tau_1 \tag{4.1-11}$$

where τ_1 is to be determined, we have that

$$\left\{ M(\theta) J_h^{-1} G^t + J_h^t G^+ \begin{bmatrix} m & 0 \\ 0 & I \end{bmatrix} \right\} \begin{bmatrix} \dot{v}_{pb} \\ \dot{\omega}_{pb} \end{bmatrix} = \tau_1 - J_h^t x_o \tag{4.1-12}$$

or

$$M_h \begin{bmatrix} \dot{v}_{pb} \\ \dot{\omega}_{pb} \end{bmatrix} = \tau_1 - J_h^t x_o .$$

Substitute (4.1-6) into the above equation, we have

$$M_h \left\{ U \begin{bmatrix} \ddot{r}_{pb} \\ \dot{\phi}_{pb} \end{bmatrix} + \dot{U} \begin{bmatrix} \dot{r}_{pb} \\ \dot{\phi}_{pb} \end{bmatrix} \right\} = \tau_1 - J_h^t x_o . \tag{4.1-13}$$

Further, let the control input τ_1 be

$$\tau_1 = M_h U \left\{ \begin{bmatrix} \ddot{r}_{pb,d} \\ \dot{\phi}_{pb,d} \end{bmatrix} - K_v \dot{e}_p - K_p e_p \right\} + M_h \dot{U} \begin{bmatrix} \dot{r}_{pb} \\ \dot{\phi}_{pb} \end{bmatrix} + J_h^t (x_{o,d} - K_I \int e_f) \tag{4.1-14}$$

and apply it to (4.1-13) to yield:

$$M_h U \left\{ \ddot{e}_p + K_v \dot{e}_p + K_p e_p \right\} = -J_h^t (e_f + K_I \int e_f). \tag{4.1-15}$$

Multiply the above equation by GJ_h^{-t}, we obtain the following equation.

$$GJ_h^{-t} M_h U \left\{ \ddot{e}_p + K_v \dot{e}_p + K_p e_p \right\} = G(e_f + K_I \int e_f) = 0. \tag{4.1-16}$$

where we have used the fact that the internal grasping forces lie in the null space of G, i.e.,

$$G(e_f + K_I \int e_f) = 0, \tag{4.1-17}$$

Since $GJ_h^{-t} M_h = GJ_h^{-t} M(\theta) J_h^{-1} G^t + \begin{bmatrix} m & 0 \\ 0 & I \end{bmatrix}$ is positive definite and U is non-singular, (4.1-16) implies that

$$\ddot{e}_p + K_v \dot{e}_p + K_p e_p = 0 \tag{4.1-18}$$

Thus, we have shown that the position error e_p can be driven to zero with proper choice of the feedback gain matrices K_v and K_p.

The last step is to show that e_f also goes to zero. If we substitute (4.1-18) into (4.1-15) and notice that J_h is nonsingular, we have the following equation.

$$e_f + K_I \int e_f = 0, \tag{4.1-19}$$

With proper choice of K_f, the above equation implies that the internal grasping force error e_f converges to zero.

Q.E.D.

4.2. Simulation

Consider the two-fingered planar manipulation system shown in Figure 12.

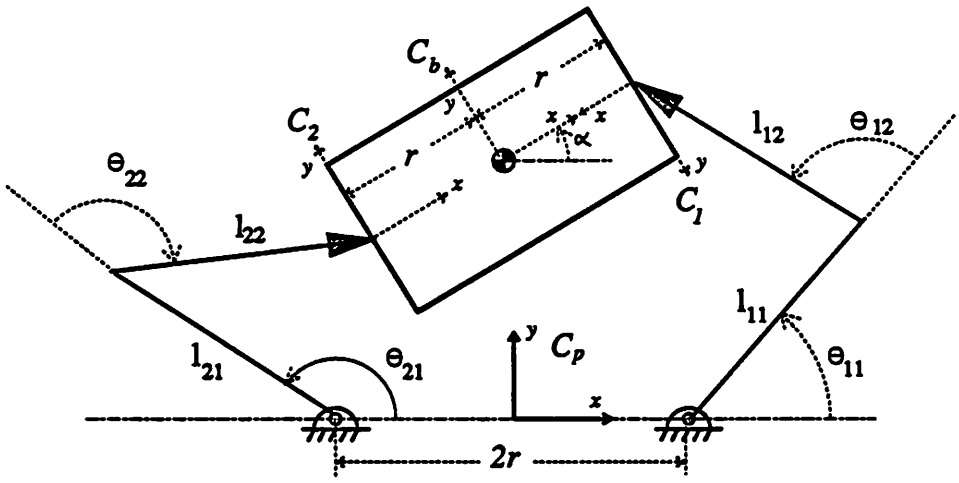

Figure 12. A two-fingered hand manipulating an object.

where the two fingers are assumed to be identical. We model the contact to be a point contact with friction. The grasp matrix and the expression for the hand Jacobian are given in (3.1-7) and (3.1-8). It has been shown in Example 3-8 that the grasp configuration in the figure is both stable and manipulable. We have simulated the system to follow the following desired trajectory of the body:

$$x(t) = c_1\sin(t), \quad y(t) = c_2 + c_1\cos(t), \quad \alpha(t) = c_3\sin(t). \tag{4.2-1}$$

The dynamic equation of the ith finger (i=1,2) used in the simulation is

$$M_i = \begin{bmatrix} m_1h_1^2+m_1d_1^2+m_2l_1^2 & m_2l_1h_2C(\theta_{i2}-\theta_{i1}) \\ m_2l_1h_2C(\theta_{i2}-\theta_{i1}) & m_2(h_2^2+d_2^2) \end{bmatrix} \tag{4.2-2}$$

$$N_i = \begin{bmatrix} m_2l_1h_2\dot{\theta}_2^2S(\theta_{i2}-\theta_{i1})+m_1gh_1S\theta_{i1}+m_2gl_1S\theta_{i1} \\ m_2l_1h_2\dot{\theta}_2^2S(\theta_{i2}-\theta_{i1})+m_2gh_2S\theta_{i2} \end{bmatrix} \tag{4.2-3}$$

where m_j = mass of the jth link, d_j=radii of gyration of jth link, h_j=the distance between the jth joint and the c.m. of the jth link. The mass matrix of the object is

$$\begin{bmatrix} m & 0 & 0 \\ 0 & m & 0 \\ 0 & 0 & I \end{bmatrix} \tag{4.2-4}$$

where m is mass of the object and I is the rotational inertial about the z axis of the object.

The simulation used a program designed to integrate differential equations with algebraic constraints. Figure 13 shows that the initial position error (in Cartesian space) diminishes exponentially as predicted by equation 4.2-18.

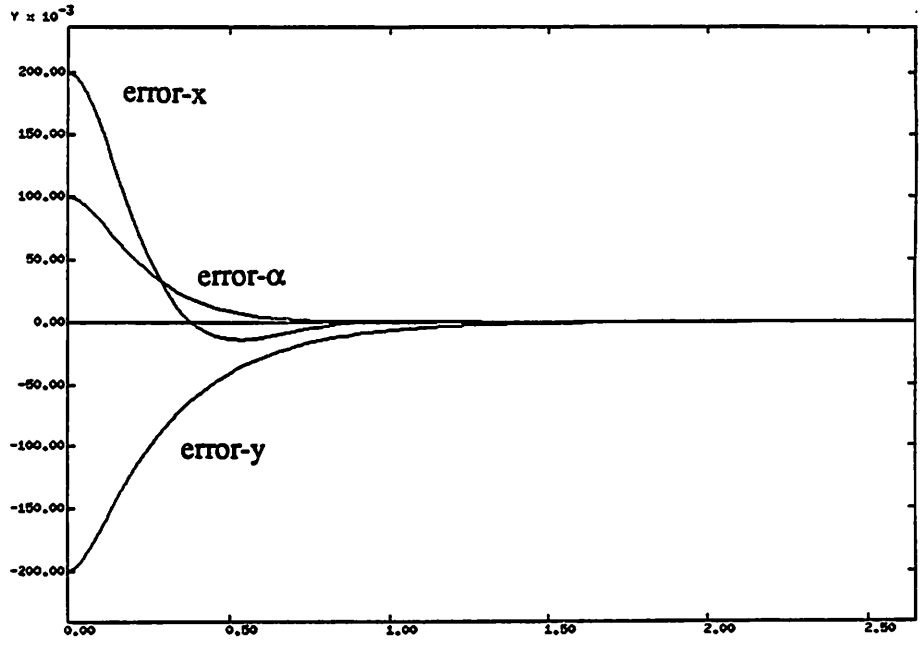

Figure 13. Position error.

The simulation was fed to a movie package (Courtesy of John Hauser) which shows the continuous motion. Figure 14 and 15 are sequences of sampled pictures from a typical simulation. In both figures, the line segment at each contact shows the magnitude and the direction of the total force that is exerted to the object by the finger. The desired grasp forces are set to 0 and 10 unit force in figure 14 and 15 respectively. Note that without the grasping force (Figure 14), the total exerted force may be away from the friction cone and consequently break the contact if this were a real experiment rather than a simulation. In related works, our colleagues, Richard Murray and Kris Pister have constructed such a two-fingered hand and are in the process of implementing this and other control laws.

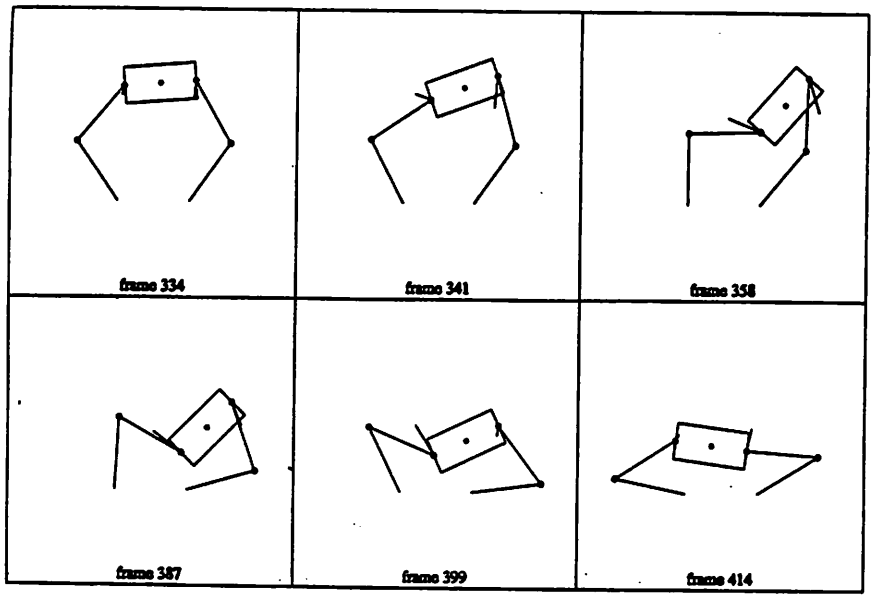

Figure 14. Simulation without internal grasping force.

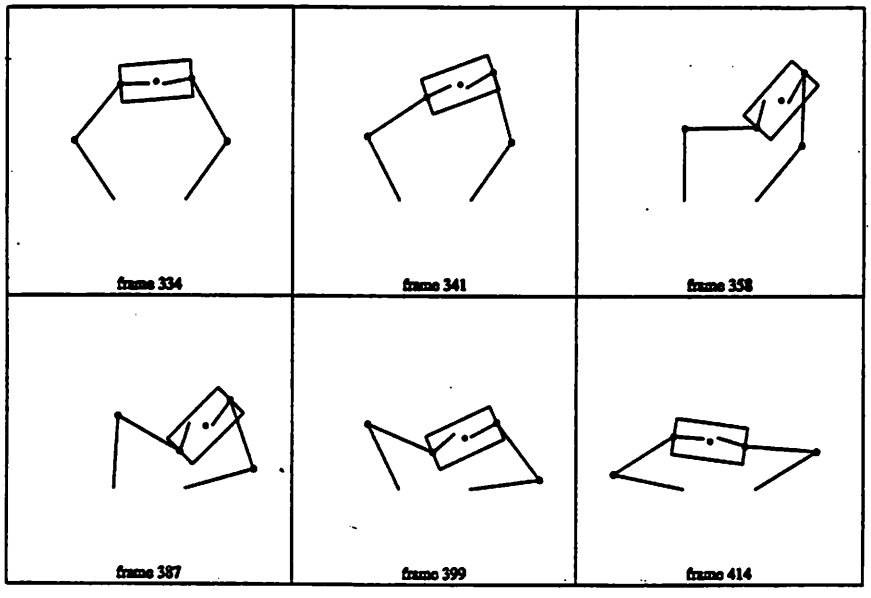

Figure 15. Simulation with 10 units of internal grasping force.

5. Concluding Remarks

We have studied techniques for the determination of grasp stability and manipulability of an object by a multifingered hand. We have also provided a control algorithm to generate the appropriate motor torques required to manipulate an object in a certain prescribed fashion. The scheme is shown to converge in the sense that the true body trajectory converges to the desired body trajectory. An application of our scheme to a planar manipulation of an object by a two-fingered hand is presented.

In future work we will study more sophisticated models for contact of a body by a multifingered hand and their implications for the schemes of this paper.

Acknowledgement

This research was supported in part by NSF under grant #DMC-8451129. We would like to thank John Hauser for performing the simulation of Figure 13 ~15, Arlene Cole, Greg Heinzinger, Richard Murrary and Kris Pister for their help in prehending a number of ideas.

References

[1] J. Kerr, "An Analysis of Multifingered Hand", Ph.D. Thesis, Stanford University, Dept. of Mechanical Engineering, December 1984.

[2] Z.X. Li and S. Sastry, "Task Oriented Optimal Grasping By Multifingered Robot Hands", to appear in *IEEE Journal of Robotics and Automation.* Also, in Proc. *1987 IEEE International Conference on Robotics and Automation*, pp389-394, and UCB ERL Memo. NO. UCB/ERL M86/43, May 1986. University of California, Berkeley.

[3] V. Nguyen, "Constructing Stable Grasps in 3-D", "Constructing Force-closure Grasps in 3-D", in Proc. *1987 IEEE International Conference on Robotics and Automation*, pp234-245, March 1987.

[4] H. Kobayashi, " Geometric Considerations for a Multifingered Robot Hand", *International Journal of Robotics Research*, Vol.4, No.1, Spring 1985, pp3-12.

[5] D. Montana, " Tactile Sensing and Kinematics of Contact", Ph.D. Thesis, Harvard University, the Division of Applied Sciences, August, 1986.

[6] M. Cutkosky, "Grasping and Fine Manipulation for Automated Manufacturing", Ph.D. Thesis, Carnegie-Mellon University, Dept. of Mechanical Engineering, January, 1985.

[7] M. Brady, J. Hollerbach, T. Johnson, T. Lozano-Perez and M. Mason, *"Robot Motion Planning and Control"*, MIT Press, 1982.

[8] Y. Nakamura, K. Nagai and T. Yoshikawa, " Mechanics of Coordinative Manipulation by Multiple Robotic Mechanisms", in Proc. *1987 IEEE International Conference on Robotics and Automation*, pp991-998.

[9] T. Yoshikawa, " Manipulability of Robotic Mechanism", Technical Report, Automation Research Laboratory, Kyoto University, Japan.

[10] J. Salisbury, " Kinematic and Force Analysis of Articulated Hands", Ph.D. Thesis, Stanford University, Dept. of Mechanical Engineering, 1982.

[11] M. Cutkosky, J. Jourdian, and P. Wright, " Skin Materials for a Robot Hand", *IEEE International Conference on Robotics and Automation*, April, 1987, Raleigh, N.C. pp1649-1654.

[12] S. Chiu, " Task Compatibility of Manipulator Postures", Technical Report, 1987. Rockwell International Science Center, Thousand Oaks, Ca. 91360

[13] J. Trinkle, "Mechanics and Planning of Enveloping Grasps", Ph.D. Thesis, 1987, Dept. of Computer and Information Science, University of Pennsylvania.

[14] Z. Ji and B. Roth, " Planning for Three-finger Tip-prehension Grasps", Tech. Report, 1987. Dept. of Mechanical Engineering, Stanford University, Ca.94305.

[15] M. Cutkosky, P. Akella, R. Howe, and I. Kao, " Grasping as a Contact Sport", Tech. Report, 1987. Dept. of Mechanical Engineering, Stanford University, Ca. 94305.

[16] H. Asada, "On the Dynamic Analysis of a Manipulator and its End Effector Interacting with the Environment", in Proc. *1987 IEEE International Conference on Robotics and Automation*, pp751-756.

[17] J. Barber and R. Volz, et al, " Automatic Two-fingered Grip Selection", in Proc. *1986 IEEE International Conference on Robotics and Automation*, pp890-896.

[18] J. Kerr and B. Roth, " Analysis of Multifingered Hands", *International Journal of Robotics Research*, Vol.4, No. 4, Winter 1986, pp3-17.

[19] S. Jacobsen, J. Wood, K. Bigger and E. Inversen, " The Utah/MIT Hand: Work in Progress", *International Journal of Robotics Research*, Vol. 4, No. 3, pp 221-250.

[20] R. Paul, *Robot Manipulators: Mathematics, Programming and Control*, PIT Press, 1981.

[21] M. DeCarmo, *Differential Geometry of Curves and Surfaces*, Prentice Hall, Inc. Englewood Cliffs, New Jersey, 1976.

[22] V. Arnold, *Classical Mechanics* 2nd Ed. 1978.

[23] Y.F. Zheng and J.Y.S. Luh, " Control of Two Coordinated Robots in Motion", in *Proc. 24th Control and Decision Conference*, pp1761-1766, 1985.

[24] T. Tarn, A. Bejczy, and X. Yuan, " Control of Two Coordinated Robots", in Proc. *1986 IEEE International Conference on Robotics and Automation*, pp1193-1202.

[25] Arimoto, " Cooperative Motion Control of Multirobot Arms or Fingers", in Proc. *1987 IEEE International Conference on Robotics and Automation*, pp1407-1412.

[26] S. Hayati, "Hybrid Position/Force Control of Multi-Arm Cooperating Robots", in Proc. *1986 IEEE International Conference on Robotics and Automation*, pp82-89, San Francisco.

[27] A. Cole, J. Hauser, and S. Sastry, "Kinematics and Control of Multifingered Hands with Rolling Contact", submitted to 1988 *IEEE International Conference on Robotics and Automation.*

Appendix A. How Does a Grasp Depend on the Local Contact Geometries?

In this appendix, we present an approach to incorporate the local contact geometries in the definition of the *effective force domain* K of a grasp map G (see Remark (2) following Definition 2-2). We will see especially in Section 3 that when the neighborhood of a contact point does not match that of the fingertip the quality of the resulting grasp will in general be inferior. Hence, using this approach in the process of automatic grasp selection (Section 3) the edges of an object can be avoided.

First, we follow the notation of [21] to review some elementary geometry of surfaces. Consider the surface shown in Figure A1 (a), which locally can be described as the graph of a differentiable function (Chapter 3, [21]).

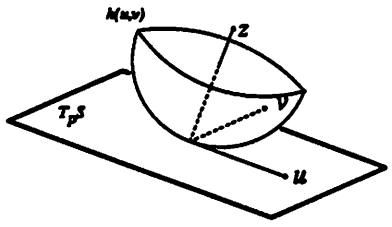

(a) A regular surface in R^3.

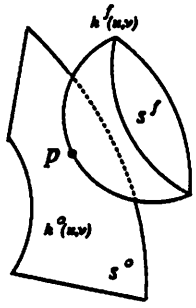

(b) A contacting surface pair in R^3.

Figure A1.

Thus, a neighborhood of a point p in S can be represented in the form $z = h(x, y), (x, y) \in U \subset R^2$, where U is an open set and h is a differentiable function with $h(0,0) = 0$, $h_x(0, 0) = 0$ and $h_y(0, 0) = 0$. Here $h_x(x, y)$ and $h_y(x, y)$ stand for the partial derivative of h with respect to x and y respectively. In other words, S locally can be parametrized by the map

$$X: U \subset R^2 \rightarrow R^3,\ X(u, v) = (u, v, h(u, v)) \tag{a-1}$$

where $u = x, v = y$. From (a-1) we obtain

$$X_u = (1, 0, h_u),\ X_v = (0, 1, h_v), X_{uu} = (0, 0, h_{uu}) \tag{a-2}$$

$$X_{uv} = (0, 0, h_{uv}),\ X_{vv} = (0, 0, h_{vv})$$

We can choose a unit normal vector at each point of $X(U)$ by the rule

$$N(q) = \frac{X_u \times X_v}{| X_u \times X_v |}(q),\ q \in X(U) \tag{a-3}$$

Thus, we have a differentiable map $N: X(U) \rightarrow R^3$ that associates to each point $q \in X(U)$ a unit normal

vector $N(q)$.

The map $N : S \rightarrow S^2$ is called the Gauss map of S. It is straightforward to verify that the Gauss map is differentiable. The differential $dN(q)$ of N at q $\in S$ is a linear map from $T_q(S)$ to $T_{N(q)}(S^2)$. Since $T_q(S)$ and $T_{N(q)}(S^2)$ are parallel planes, $dN(q)$ can be looked upon as a linear map on $T_q(S)$. The matrix representation of the linear map $dN(q)$ is a 2 by 2 matrix given by [DeCarmo, Chapter 3]

$$dN(q) = \begin{bmatrix} a_{11} & a_{12} \\ a_{21} & a_{22} \end{bmatrix} \tag{a-4}$$

where

$$a_1 = \frac{fF - eG}{EG - F^2}, \quad a_{21} = \frac{eF - fE}{EG - F^2}$$
$$a_{12} = \frac{gF - fG}{EG - F^2} \quad a_{22} = \frac{fF - gE}{EG - F^2}$$

and

$$E = \langle X_u, X_u \rangle, \; F = \langle X_u, X_v \rangle, G = \langle X_v, X_v \rangle$$

$$-e = \langle N_u, X_u \rangle, \; -f = \langle N_u, X_v \rangle, \; -g = \langle N_v, X_v \rangle$$

Remark: The determinant of $dN(q)$ is called the Gauss curvature of the surface at the point q.

We then consider a contacting surface pair shown in Figure A1 (b). Here S_f stands for the fingertip, S_o for the object and p is the point of contact. We may assume without loss of generality that the possible region of contact for the fingertip is fixed and is denoted by Q, and before the fingertip deforms the initial point of contact p is at the center of Q. We further assume that both surfaces are differentiable and the edges of a surface can be accounted for by taking the limit of a differentiable surface. Consequently, we can choose two maps X^f and X^f to parametrize S_f and S_o by

$$X^f : U \subset R^2 \rightarrow S^f \subset R^3; \; X^f(u,v) = (u, v, h^f(u,v)) \tag{a-5a}$$

and

$$X^o : U \subset R^2 \rightarrow S^o \subset R^3; \; X^o(u,v) = (u, v, h^o(u,v)) \tag{a-5b}$$

where h^f and h^o are both differentiable functions. Assume that X^o is defined on $(X^f)^{-1}(Q)$ and and define the relative curvature form of the contacting surface pair at a point in $(X^f)^{-1}(Q)$ to be

$$dN^o + dN^f \tag{a-6}$$

The surface conforming coefficient c(p, Q) of S_o with respect to S^f over the region Q is defined by

$$c(p,Q) = \int\int_{(X^f)^{-1}(Q)} \| \, dN^o + dN^f \, \| \, du \, dv \tag{a-7}$$

where $\| \cdot \|$ is the l_2 induced matrix norm.

The surface conforming coefficient c is a function of the contact point and the local geometries of the contact surface pair at p. If two surfaces have contact of order 2 over $(X^f)^{-1}$ (Q) then c is identically zero and the two surfaces agree. We define such a contact point to be a very regular point. But, as the two surfaces differ from each other over Q the furface conforming coefficient will be nonzero. In the limiting case when the point of contact is at the edges of an object c increases to infinity and the point of contact is defined to be "very irregular". Consequently, tangential component frictional forces or torional frictional forces are difficulty to apply over the gripped object.

Finally, we use the information contained in c(p, Q) to modify the definition of the effective force domain K_i of the contact map (2.2-2) as follows: choose a montonically decreasing function $g: [0, \infty) \rightarrow [0, 1]$ such that

$$g(0) = 1, \; and \; \lim_{n \rightarrow \infty} g(n) = 0 \tag{a-8}$$

define the effective Coulomb, and/or torsional frictional coefficient μ_e by

$$\mu_e = f(c)\,\mu_0 \tag{a-9}$$

where μ_0 is the nominal frictional coefficient measured when the pair of surfaces agree, and apply this μ_e to the definition of K_i.

Remark: Note that if the two surfaces agree μ_e is just the nominal frictional coefficient and the frictional forces will be transmitted as predicted by the point contact model. If the two surfaces disagree, or p is a very irregular point, the frictional forces will be transmitted also according to μ_e. This shows that under this modification the point contact model is always valid.

Appendix B. Coordinated Control for Redundant Fingers

In this appendix, we supplement to Theorem 4-1 the control algorithm for redundant fingers, where the number of joints m_i, $i = 1, ..., k$ is greater than the number of constrained directions n_i, $i = 1,... k$. In many industrial applications, several robots which often have more than three degree of freedoms are integrated to maneuver a massive load. Under the frictional point contact model such a system is redundant. The dynamic distinction of a redundant hand from a nonredundant hand is the internal motion given by $\ddot{\theta}_0$ in (4.0-4). We claim that the following control law will achieve the desired control objective for a hand with redundant:

$$\tau = N(\theta, \dot{\theta}) + J_h^t\, G^+ \begin{bmatrix} \omega_{pb} \times m v_{pb} \\ \omega_{pb} \times I\, \omega_{pb} \end{bmatrix} - M\, J_h^+ \dot{J}_h\, \dot{\theta} + M J_h^+ (J_h M^{-1} J_h^t)\, M_h\, \dot{U} \begin{bmatrix} \dot{r}_{pb} \\ \dot{\phi}_{pb} \end{bmatrix} \tag{b-1a}$$

$$+ M J_h^+ (J_h M^{-1} J_h^t)(\, x_{o,d} - K_I \int e_f\,) + M J_h^+ (J_h\, M^{-1}\, J_h^t) M_h\, U \left\{ \begin{bmatrix} \ddot{r}_{pb,d} \\ \dot{\phi}_{pb,d} \end{bmatrix} - K_v\, \dot{e}_p - K_p\, e_p \right\}$$

where

$$M_h = (J_h\, M^{-1}\, J_h^t)^{-1}\, G^t + G^+ \begin{bmatrix} m & 0 \\ 0 & I \end{bmatrix} \tag{b-1b}$$

Remark: Please compare (b-1) with (4.1-9) and observe that the M_h is different here.

To see this, we use (4.0-4) and (4.0-8) in (4.1-3) and suppress the θ dependence of M to get

$$M \left\{ J_h^+ G^t \begin{bmatrix} \dot{v}_{pb} \\ \dot{\omega}_{pb} \end{bmatrix} - J_h^+ \dot{J}_h\, \dot{\theta} \right\} + M\, \ddot{\theta}_0 + N(\theta, \dot{\theta}) = \tau$$

$$- J_h^t \left\{ G^+ \begin{bmatrix} m & 0 \\ 0 & I \end{bmatrix} \begin{bmatrix} \dot{v}_{pb} \\ \dot{\omega}_{pb} \end{bmatrix} + G^+ \begin{bmatrix} \omega_{pb} \times m v_{pb} \\ \omega_{pb} \times I\, \omega_{pb} \end{bmatrix} \right\} - J_h^t\, x_0 \tag{b-2}$$

Comparing to (4.1-10) we see that there is an extra term $M\, \ddot{\theta}_0$ in (b-2), as well as J_h^{-1} is replaced by the generalized inverse J_h^+.

Choosing the following control input:

$$\tau = N(\theta, \dot{\theta}) + J_h^t G^+ \begin{bmatrix} \omega_{pb} \times m v_{pb} \\ \omega_{pb} \times I\, \omega_{pb} \end{bmatrix} - M\, J_h^+ \dot{J}_h\, \dot{\theta} + \tau_1 \tag{b-3}$$

where τ_1 is to be determined, we have that

$$\left\{ M J_h^+ G^t + J_h^t\, G^+ \begin{bmatrix} m & 0 \\ 0 & I \end{bmatrix} \right\} \begin{bmatrix} \dot{v}_{pb} \\ \dot{\omega}_{pb} \end{bmatrix} + M\, \ddot{\theta}_0 = \tau_1 - J_h^t\, x_0 \tag{b-4}$$

Multiplying the above equation by $J_h\, M^{-1}$ and using the fact that $J_h\, \ddot{\theta}_0 = 0$ yields

$$\left\{ G^t + J_h M^{-1} J_h^t \, G^+ \begin{bmatrix} m & 0 \\ 0 & I \end{bmatrix} \right\} \begin{bmatrix} \dot{v}_{pb} \\ \dot{\omega}_{pb} \end{bmatrix} = J_h M^{-1} \tau_1 - J_h M^{-1} J_h^t \, x_0 \tag{b-5}$$

Since J_h is onto, $J_h M^{-1} J_h^t$ is nonsingular and we can further multiply (b-5) by $(J_h M^{-1} J_h^t)^{-1}$ to obtain

$$\left\{ (J_h M^{-1} J_h^t)^{-1} G^t + G^+ \begin{bmatrix} m & 0 \\ 0 & I \end{bmatrix} \right\} \begin{bmatrix} \dot{v}_{pb} \\ \dot{\omega}_{pb} \end{bmatrix} = (J_h M^{-1} J_h^t)^{-1} \, J_h M^{-1} \tau_1 - x_0 \tag{b-6}$$

Substituting (4.1-6) into (b-6) and choosing the following remaining control input for τ_1 we obtain

$$\tau_1 = M J_h^+ (J_h M^{-1} J_h^t) \left\{ M_h U \left[\begin{bmatrix} \ddot{r}_{pb,d} \\ \dot{\phi}_{pb,d} \end{bmatrix} - K_v \, \dot{e}_p + K_p \, e_p \right] + M_h \dot{U} \begin{bmatrix} \dot{r}_{pb} \\ \dot{\phi}_{pb} \end{bmatrix} + (x_{0,d} - K_I \int e_f \,) \right\} \tag{b-7}$$

and

$$M_h U \{ \ddot{e}_p + K_v \, \dot{e}_p + K_p e_p \} = -(e_f + K_I \int e_f) \tag{b-8}$$

Multiplying (b-8) by G and using the fact that $G(e_f + K_I \int e_f) = 0$ we obtain that

$$G \; M_h U \{ \ddot{e}_p + K_v \, \dot{e}_p + K_p \, e_p \} = 0 \tag{b-9}$$

Since $G \; M_h = G (J_h \; M^{-1} J_h^t)^{-1} \, G^t + \begin{bmatrix} m & 0 \\ 0 & I \end{bmatrix}$ and U are both nonsingular (b-9) immediately implies that

$$\ddot{e}_p + K_v \, \dot{e}_p + K_p \, e_p = 0 \tag{b-10}$$

which shows that the position error e_p can be driven to zero by proper choice of the feedback gain matrices K_v and K_p.

On the other hand, using (b-10) in (b-8) we finally obtain that

$$e_f + K_I \int e_f = 0 \tag{b-11}$$

which shows that the internal grasping force error can also be driven to zero by proper choice of the forec integral gain matrix K_I.